CZECH TECHNICAL UNIVERSITY IN PRAGUE
ČESKÉ VYSOKÉ UČENÍ TECHNICKÉ V PRAZE

FACULTY OF ELECTRICAL ENGINEERING
DEPARTMENT OF MICROELECTRONICS

FAKULTA ELEKTROTECHNICKÁ
KATEDRA MIKROELEKTRONIKY

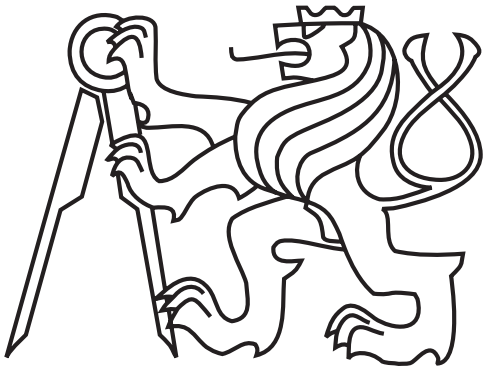

RADIATION RESISTANCE MEASUREMENT ON NANOSATELLITE MINICUBE MISSION QB50

MASTER'S THESIS
DIPLOMOVÁ PRÁCE

2015 Bc. VERONIKA STEHLÍKOVÁ

CZECH TECHNICAL UNIVERSITY
IN PRAGUE
ČESKÉ VYSOKÉ UČENÍ TECHNICKÉ V PRAZE

FACULTY OF ELECTRICAL ENGINEERING
DEPARTMENT OF MICROELECTRONICS

FAKULTA ELEKTROTECHNICKÁ
KATEDRA MIKROELEKTRONIKY

RADIATION RESISTANCE MEASUREMENT ON NANOSATELLITE MINICUBE MISSION QB50

MĚŘENÍ RADIAČNÍ ODOLNOSTI UHLÍKOVÉHO KOMPOZITU NA NANOSATELITU MINICUBE MISE QB50

MASTER'S THESIS
DIPLOMOVÁ PRÁCE

AUTHOR — Bc. VERONIKA STEHLÍKOVÁ
AUTOR PRÁCE

SUPERVISOR — Ing. LADISLAV SIEGER, CSc.
VEDOUCÍ PRÁCE

Prague 2015

České vysoké učení technické v Praze
Fakulta elektrotechnická

katedra mikroelektroniky

ZADÁNÍ DIPLOMOVÉ PRÁCE

Student: **Bc. S T E H L Í K O V Á Veronika**

Studijní program: Komunikace, multimédia a elektronika
Obor: Elektronika

Název tématu: **Měření radiační odolnosti uhlíkového kompozitu na nanosatelitu miniCube mise QB50**

Pokyny pro vypracování:

1) Prostudujte problematiku měření radiační odolnosti ve vesmíru.
2) Porovnejte vlastnosti dostupných křemíkových XRB Diod a CdTe detektorů pro detekci RTG záření v závislosti na jeho energii.
3) Realizujte nízkošumové a nízkopříkonové zapojení pro měření na Payloadu nanosatelitu miniCube mise QB50.
4) Ověřte a zhodnoťte funkčnost zapojení a jeho spolehlivost.
5) Proveďte kalibraci a měření navrženého Payloadu v rozsahu 10 keV - 500 keV v závislosti na radiačním stínění
6) Zhodnoťte vhodnost použitých postupů, poznatky a jejich možnosti dalšího využití.

Seznam odborné literatury:

1. ESA Radiation: Radiation Design Handbook. Section 3: The Radiation Environment [online]. Noordwijk: ESA Publications Division, 1993 [cit. 2014-10-06]. Available from www: https://escies.org/download/webDocumentFile?id=59313.
2. Tavlet, M.; Fontaine, A.; Schönbacher, H. Compilation of radiation damage test data, pt.2, 2nd ed.; Geneva : CERN, 1998. - 173 p., 1998.
3. E.L.Dereniak, D.G.Growe: Optical radiation detectors, John Wiley & Sons, 1984.

Vedoucí: **Ing. Ladislav Sieger, CSc.**

Platnost zadání: 31. 8. 2016

L.S.

prof. Ing. Miroslav Husák, CSc.
vedoucí katedry

prof. Ing. Pavel Ripka, CSc.
děkan

V Praze dne 18. 2. 2015

Czech Technical University in Prague
Faculty of Electrical Engineering

Department of Microelectronics

Master's Thesis Assignment

Student: **Bc. S T E H L Í K O V Á Veronika**

Study program: Communication, Multimedia and Electronics
Focused: Electronics

Topic:

Radiation resistance measurement on nanosatellite miniCube mission QB50

Instructions:

1) Study the problematic of radiation resistance measurement in space.
2) Compare the properties of silicon XRB diodes and CdTe detectors for detection of RTG radiation in dependence on its energy.
3) Implement a low noise and low power wiring for measurement on Payload of nanosatellite miniCube mission QB50.
4) Check and evaluate the functionality of the wiring and its reliability.
5) Make the calibration and measurement of the designed Payload in the range of 10 keV – 500keV in dependence on the radiation shielding.
6) Evaluate the suitability of used procedures, findings and the possibility of their further use.

References:

[1] ESA Radiation: Radiation Design Handbook. Section 3: The Radiation Environment [online]. Noordwijk: ESA Publications Division, 1993 [cit. 2014-10-06]. Available from www: https://escies.org/download/webDocumentFile?id=59313.

[2] Tavlet, M.; Fontaine, A.; Schönbacher, H. Compilation of radiation damage test data, pt.2, 2nd ed.; Geneva : CERN, 1998. - 173 p., 1998.

[3] E.L.Dereniak, D.G.Growe: Optical radiation detectors, John Wiley & Sons, 1984.

Supervisor: **Ing. Ladislav Sieger, CSc.**

Assignment validity: 31. 8. 2016

L.S.

prof. Ing. Miroslav Husák, CSc.
Head of department

prof. Ing. Pavel Ripka, CSc.
Dean

In Prague, 18. 2. 2015

ABSTRACT

The new carbon fiber material will be tested as a shielding material for future usage on large satellites. The Cube carries three PIN diodes and one CdTe detector. PIN diodes are shielded with wolfram from behind to eliminate secondary radiation generated inside the probe. Active layers are orientated to the free space and each one of them has different shielding. The first is protected by wolfram plate, the second by the tested carbon fiber and the last does not have any shielding. Signal from diodes is amplified, led to another board and digitalized. Energy of signal is expected to start around 10 keV. Data from the new material measurement will be compared to reference diodes and final results will be processed on Earth. This thesis is about measuring design and and testing of new methods of quality assessment of a new shielding material.

KEYWORDS

Radiation durability, PIN diode, CdTe detector, carbon-fibre composite, magnetosphere, CubeSat, QB50, space, low-noise amplifier

ANOTACE

Tato diplomová práce se zabývá posouzením vhodnosti nově vyvinutého materiálu pro použití v podmínkách vesmírného prostoru z hlediska schopnosti chránit sondu před zářením. Družice ponese tři PIN diody a CdTe detektor. PIN diody budou stíněny různými způsoby - wolframem, testovaným karbonovým materiálem a třetí bude čelit volnému prostoru nechráněna. Signál z diod bude zesilován, digitalizován a porovnáván s referencemi. Očekáváme, že zachycované energie částic budou začínat na 10 keV. Výsledky měření budou zaslány k vyhodnocení na pozemskou stanici.

KLÍČOVÁ SLOVA

Radiační odolnost, PIN dioda, CdTe detektor, uhlíkový kompozit, magnetosféra, CubeSat, QB50, space, nízkošumový zesilovač

STEHLÍKOVÁ, Veronika. *Radiation resistance measurement on nanosatellite miniCube mission QB50*: master's thesis. Prague: Czech Technical University in Prague, Faculty of Electrical Engineering, Department of Microelectronics, 2015. 59 p. Supervised by Ing. Ladislav Sieger, CSc.

ACKNOWLEDGEMENT

I would like to express my thanks my mentor Ing. Ladislav Sieger, CSc. and Ing. Milan Petřík for professional guidance, Prof. Kazuo Yana for assistance during summer internship at Hosei University, my family, which supports me everytime and also my dear colleagues, who were working on this project with me and were priceless.

DECLARATION

I declare that I have written my master's thesis on the theme of "Radiation resistance measurement on nanosatellite miniCube mission QB50" independently, under the guidance of the master's thesis supervisor and using the technical literature and other sources of information which are all quoted in the thesis and detailed in the list of literature at the end of the thesis.

As the author of the master's thesis I furthermore declare that, as regards the creation of this master's thesis, I have not infringed any copyright. In particular, I have not unlawfully encroached on anyone's personal and/or ownership rights and I am fully aware of the consequences in the case of breaking Regulation § 11 and the following of the Copyright Act No 121/2000 Sb., and of the rights related to intellectual property right and changes in some Acts (Intellectual Property Act) and formulated in later regulations, inclusive of the possible consequences resulting from the provisions of Criminal Act No 40/2009 Sb., Section 2, Head VI, Part 4.

In Prague, July 31, 2015

.....

author's signature

Contents

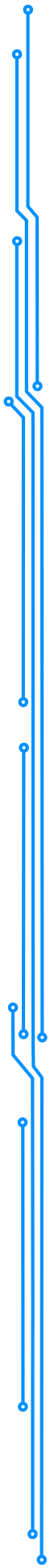

List of Figures

List of Tables

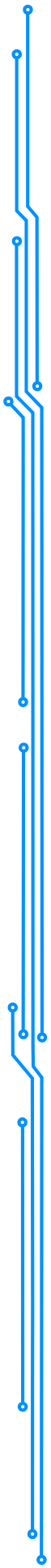

List of Acronyms

A/D
Analog to Digital

Am
Americium

Ba
Barium

Cd
Cadmium

CdTe
Cadmium-Telluride

CERN
European Organization for Nuclear Research

CMOS
Complementary Metal–Oxide Semiconductor

Co
Cobalt

CPLD
Complex Programmable Logic Device

Cs
Cesium

DST
Disturbance Storm Time

EMC
Electromagnetic Compatibility

FFT
Fast Fourier Transform

FIPEX
Flux-Φ-Probe Experiment

GPS
Global Positioning System

Hg
Mercury

HM
Health Monitoring

I
Iodine

I2C
Inter-Integrated Circuit

IR
Infrared

ISS
International Space Station

IST
Inovative Sensor Technology

LHC
Large Hadron Collider

Ni
Nickel

Np
Neptunium

OBC
On Board Computer

PCB
Printed Circuit Board

PWR
Power

SMD
Surface Montage Device

Te
Telluride

THT
Through Hole Technology

TTS
Thin-film Technology Service

UV
Ultraviolet

XRB
X-Ray Background

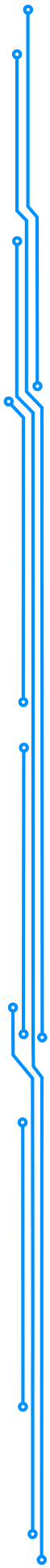

List of Symbols

Φ	Electron flux (W)
Θ	Scattering angle (°)
ϵ	Energy to create conductive pair (eV)
λ	Wavelength (m)
μ_0	Permeability of vacuum $1.26 \cdot 10^{-6} (\mathrm{H} \cdot \mathrm{m}^{-1})$
τ	Decay time (s)
τ	Value of minority carriers lifetime before irradiation (s)
τ_0	Value of minority carriers lifetime after irradiation (s)
B	Magnetic induction (T)
c	Speed of light $299\,792\,458 (\mathrm{m} \cdot \mathrm{s}^{-1})$
C_f	Feedback capacitor (F)
chnl	Channel (−)
E	Energy of particle (eV)
E	Energy of photon (eV)
E	Defined value of energy (eV)
e	The charge of one electron $1.602\,176 \cdot 10^{-19} (\mathrm{C})$
E_s	Energy of photon after scattering (eV)
E_{ch}	Energy per channel (eV)
E_{max}	Maximal energy of released electron (eV)
f	Frequency (Hz)
H	Magnetic field intensity $(\mathrm{A} \cdot \mathrm{m}^{-1})$
h	Planck's constant $4.135\,667 \cdot 10^{-15} (\mathrm{J} \cdot \mathrm{s})$
h_ν	Energy of impacting photon (eV)
$h_{\nu 0}$	Energy to release an electron (eV)
K_τ	Minority carrier lifetime damage constant $(\mathrm{s} \cdot \mathrm{W}^{-1})$
m	Weight (kg)
N	Number of channel (−)
Q_D	Charge released by detector (C)

Q_P	Gain of preamplifier (C)
R_f	Feedback resistor (Ω)
S	Cross-section, area (m^2)
t	Time (s)
U_N	Noise voltage (V)
V_0	Amplitude of output voltage (V)

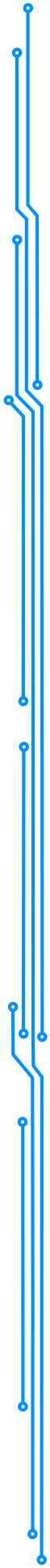

1 QB50 mission

Project VZLUsat-1 in which I am participating in is an international mission with a goal to launch small satellites to low orbit. Creating a large device such as Global Positioning System (GPS) or a meteorological satellite is a difficult task, which requires a lot of planning, work and funding. Designing such machines requires testing of materials and equipment in conditions, that are to be expected in space. These conditions cannot be simulated on test sites on Earth in full extent. It is possible to put the device into a vacuum chamber, expose it to high overload and perform other tests, but unexpected conditions still may occur during the flight.

Due to these reasons, it is very important for a mission to use reliable materials, parts and procedures. Trying anything new on such a precious device is too risky and can lead to mission failure, so it is a common practice to use technologies from the last century for high-end space research.

Project QB50 has a potential to change this situation. In this project, there are working research groups from whole world, which can develop a small, testing satellite. It is a good opportunity for students to try design procedures in unusual conditions and to experience research in a team of professionals, who can teach them many practical knowledge. And it is a great opportunity for companies to try out new materials and devices. It's possible to send untested new materials or parts on orbit, measure their behaviour in real space conditions, get data to the surface and find out, if these solutions will be usable for future experiments. So it is a way how to prove that modern technologies are suitable to be used later for regular missions and to increase lifetime and reliability of large satellites.

1.1 Goals of mission

The QB50 project is an enabler for harmonization and standardization of the CubeSat platform and to achieve an affordable access to space for small research space missions and planetary exploration. The confirmed launch date is February 1, 2016 from Brazil.

One of objectives of the QB50 project is to carry out measurement in lower thermosphere. Each of the satellites must carry one of the prescribed experiments

and measure data for the agency – rest of weight and devices can be individual. Our satellite has FIPEX on board. This shortcut stands for Flux-Φ-Probe Experiment and is mentioned later.

Lower thermosphere, between 200-380 km, is the least explored layer of atmosphere, because previous missions spent only tens of minutes in the region of interest and were carrying single-point experiments. Nowadays, the explorations are held by sounding rockets during their passing through atmosphere (only a few minutes long), by Earth observing probes, which have higher orbit and which usually scan atmosphere and by lidars and radars on the ground. Last two methods have a disadvantage, because rarefied atmosphere in the lowest thermosphere has low ability to reflect, so the returned signal is weak. QB50, making in-situ measurements, will be complementary to these other methods. From its results will benefit all atmospheric models and their users.

Compared to this, QB50 satellites are expected to work for several months and will carry out multiple-point in-situ measurements. Our VZLUsat-1 consists of two units, which means with dimensions of 10x10x20 cm. On orbit, the top part of satellite will fork out optics – lobster eye and additive solar panels. The direction of the probe's flight is not completely passive, it may be slightly corrected using interaction between Earth's magnetic field and magnetic field of positioning coils of the probe. As seen in the picture Fig. 1.1, payloads are situated inside the body of probe one above the other and they are interconnected. Whole satellite is controlled by a CPU on On Board Computer (OBC) board. Individual Payloads have their own microcontrollers, which drives only one appropriate task and communicate with OBC board. One of OBC's important tasks is to coordinate measurements and perform only one at a time. Power supply for entire satellite is only 2 W, so payloads cannot run simultaneously.

Measured data will be send to the station in Pilsen two times a day. Level of orbital processing is different for each task, but amount of data will be limited and transmission time will be short, expected time in case of ideal conditions is ten minutes. The best option is to process all calculations on orbit and send only the final results. One way how to get more information in more frequent contacts is to make our project attractive for radioamateurs. They could receive signal from the satellite and also coded data, which they could then send to us. Of course, this is only a theory, we do not know if we could use it and it would depend on goodwill of the radioamateurs.

1.2 CTU task

Me and my colleagues are working on three Payloads. Ondřej Nentvich's thesis *Measurement of changing mechanical properties of carbon composite on nanosatellite miniCube mission QB50* discusses measurement of aging a new material, carbon fiber, including design and program implementation on chip with FreeRTOS. Martin Urban in his thesis *Measurement of evaporation and evaluation of changes of the mechanical properties of carbon composite on nanosatellite miniCube mission QB50* describes problematic of finding resonance frequency by Fast Fourrier Transformation for damping signal processing and of measuring humidity and temperature on orbit. And finally, I am working on finding the best way how to measure radiation doses, spectre, energy of photons and radiation hardness of new materials and parts on VZLUSat-1.

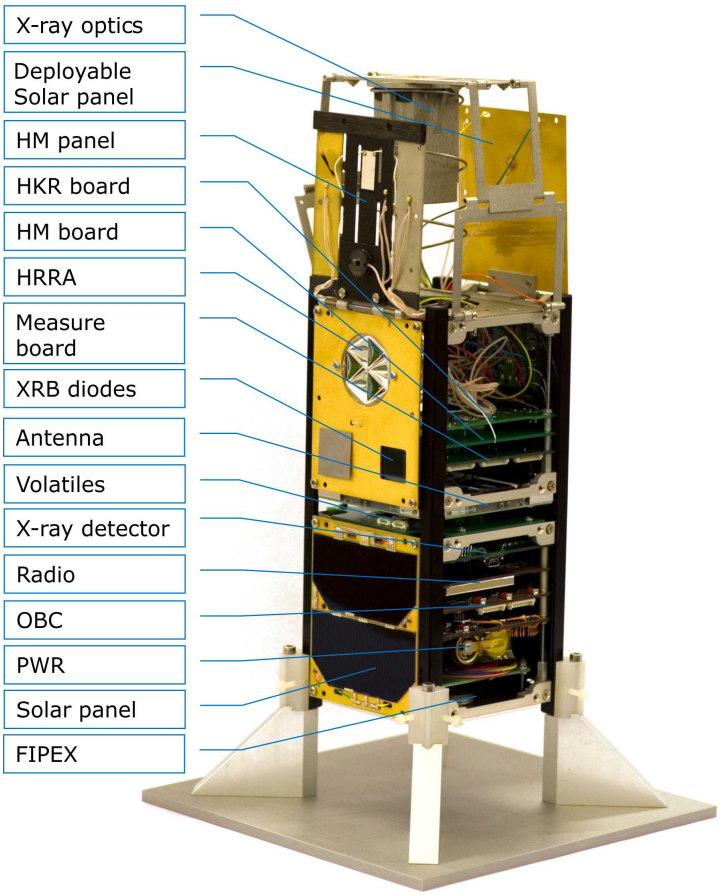

Fig. 1.1: VZLUSat-1 - placement of boards and measurements [**?**]

Measuring will be repeated every five minutes, information about radiation and current temperature will be recorded. Due to changing shape of orbit and altitude of the satellite, we could get quite complex image of low-orbit radiation environment around our planet. We will also study the effect of different shielding and compare it. One of the goals is to test the same material which is studied in Martin Urban's and Ondřej Nentvich's thesis for its qualities and potential for shielding radiation impressible silicone devices.

1.3 VZLUSat-1 – boards and functions

The satellite consists of measuring board stacked one above the other, as can be seen in Fig. 1.1. Small teams are working on individual tasks, in this subsection I am going to describe the most important parts as they are placed in our probe from top to the bottom.

1.3.1 X-Ray Optics and Medipix

The forkable out part is carrying X-Ray optics which should look into the Sun. This optic is Lobster eye type, a system of narrow shafts with right angles and straight walls. The picture appears due to reflection, not refractions as in classic optical lenses, as illustrated in Fig. 1.2. Focal length is approximately 20 cm and

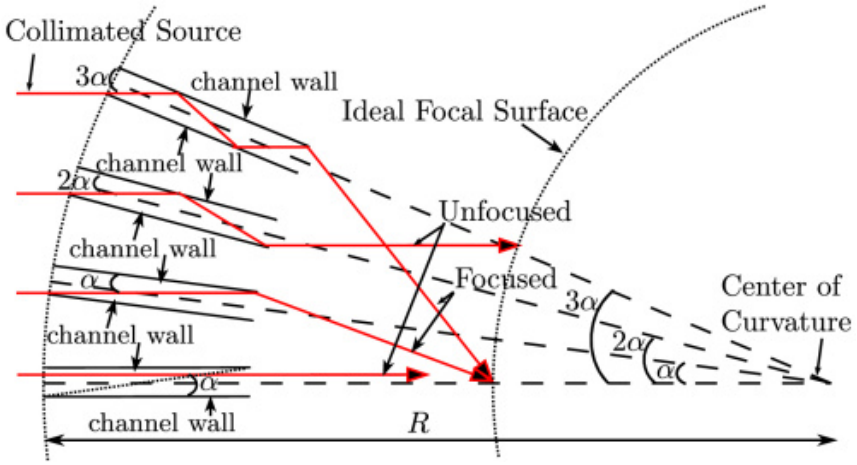

Fig. 1.2: Lobster eye - illustration of reflections and focusing [1]

there are square holes in all the boards between optics and Medipix chip itself. To detect if the orientation is right, there are three sensors for that purpose, one Infrared (IR) and two Ultraviolet (UV). One of the UV diodes has wide action radius and it

is looking for the Sun. The second one has narrover field and it gets more precise position of the Sun. When the sensors have signal which is strong enough, Medipix will switch on. Madipix is a Complementary Metal–Oxide Semiconductor (CMOS) silicon detector for low-energy X-Rays, approximately 1 – 20 keV. Originally, it was developed for Large Hadron Collider (LHC) in European Organization for Nuclear Research (CERN), nowadays it is used also for scanning soft tissues as a medical instrument.

1.3.2 Solar cells and power supply

The power supply consists of solar panels (solid and deployable) and power board Power (PWR), which provides stabilized voltages of 5 V and 3.3 V. Solar panels are the latest generation, they have three layers - InGaP, GaAs and Ge on Germanium underlay. Each of these layers absorbs different wavelengths, form UV to IR. Effectiveness for orbital conditions, that means power density of 1367 W/m^2, is 30 %. The solar panels will also receive Earth albedo and Earth infra-red radiation, as seen in Fig. 1.3

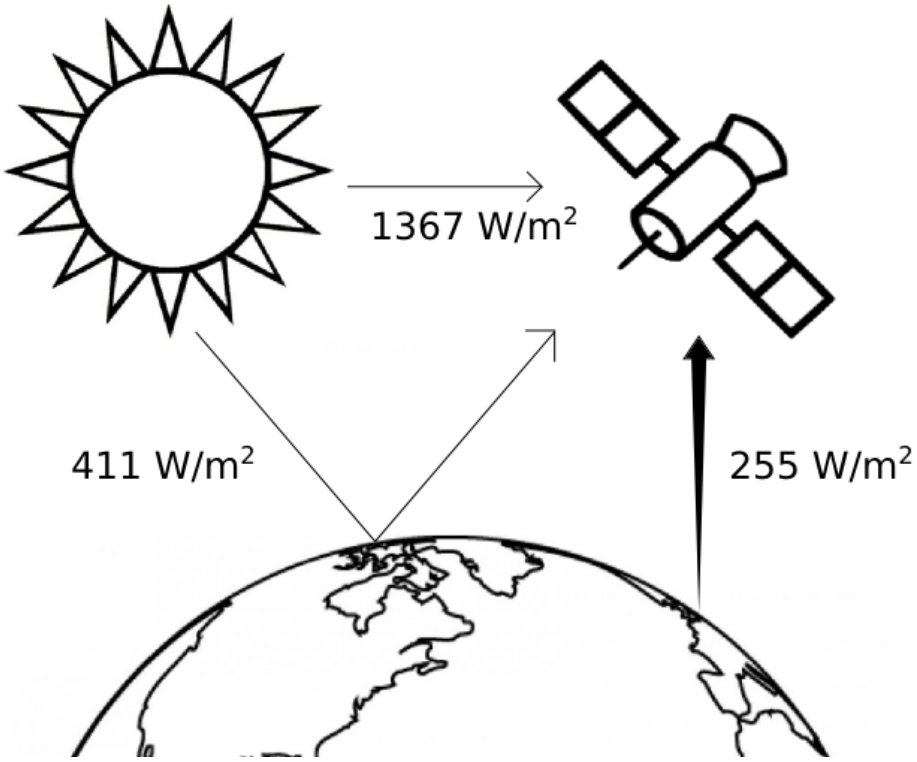

Fig. 1.3: Power densities of different sources on the orbit

Area of one solar panel is approximately 30 cm^2. Each od them can generate up to 2.4 V and 500 mA. Board has two backup lithium accumulators, used when

the probe is on the dark side of Earth. Because used type of accumulators is sensitive to undervoltage, the board detects voltage value and if it drops under the critical value, all other boards are cut off and PWR waits for better conditions. It then turns the probe on again, including the controlling OBC board.

1.3.3 Health monitoring panel and board

This measurement studies influence of mechanical stress on tested carbon-fibre material and heat transmission properties. In the middle of the board is a cantilever. A permalloy and a coil are placed on its free end. The coil will cause oscillations of the cantilever. When the beam is excited, then its oscillations are measured by piezo and results evaluated by Fast Fourier Transform (FFT). If the mechanical properties change, there may be a visible difference in resonance frequency, which is the result of FFT. There are also six thermometers on HM panel, which measure thermal transmission of surface evaporated layers of Nickel and Gold and carbon-fibre material. As in the rest of the probe, these sensors are PT 1000 type. More details about this board are in my colleague Ondřej Nentvich's thesis [2].

1.3.4 HKR board

This board in last version carries only system of locking wires, which will burn off on the orbit. Then will be released the folding part of the spacecraft carrying the X-ray optics.

1.3.5 Hollow retro reflector array

This panel carries corner reflectors and its goal is help to determine the position of the probe more accurately. Corner reflection consists of three mutually perpendicular mirrors. This arrangement reflects incoming ray ever back to its source, regardless of the rotation of mirrors.

1.3.6 Measure board with attached XRB board

The goal of this measurement is to determine the quality of radiation shielding of new carbon-fibre material. Measure board carries Cadmium-Telluride (CdTe) detector, Analog to Digital (A/D) converters, Complex Programmable Logic Device (CPLD) and microprocessor unit.

Three identical XRB diodes with different shielding are mounted on the XRB board for X-Ray measurements. This is the board, which will be mainly discussed further.

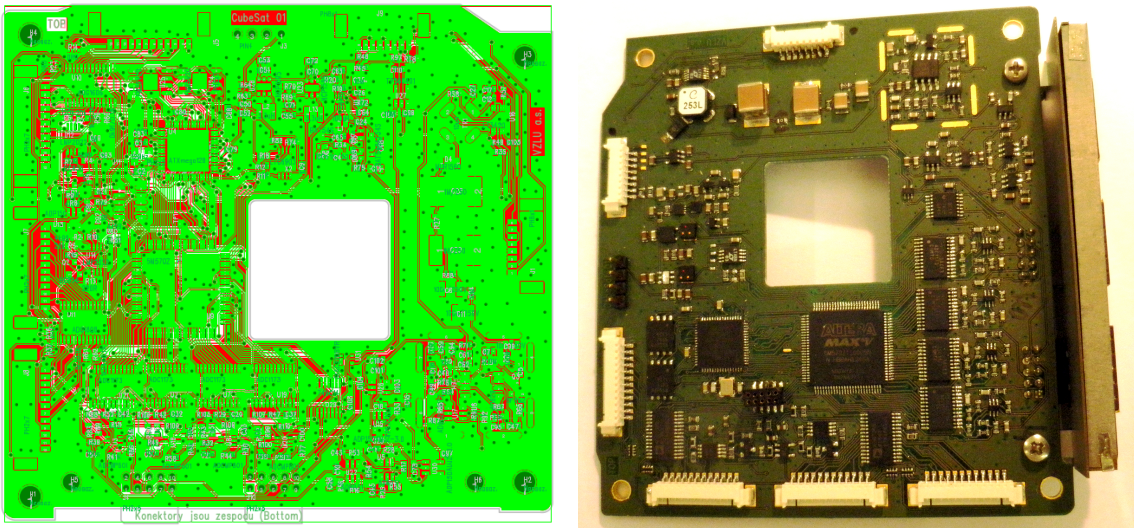

(a) Measure board - layout

(b) Measure board - mounted

Fig. 1.4: Measure board [3]

1.3.7 Volatiles board

Volatiles board serves for measurement of residual humidity from the probe, especially from tested carbon-fibre composite. This humidity will evaporate in vacuum, particularly in the first hours after launch. There are three type of sensors. Two pairs of HYT271 and HYT 939 from IST company, situated on both sides of Volatiles board. Third sensor is HAL2 from TTS which is sensitive not only to humidity, but to other gases as well. All these sensors communicate directly with OBC board, using Inter-Integrated Circuit (I2C) bus. Evaporation measurements are a goal of Martin Urban's thesis [4].

1.3.8 Radio board

Radio board provides connection with Earth and transmission of results to the station or new configurations to the orbit. This board was developed at the University of West Bohemia in Pilsen, they will also download data and process some of the results. Used transfer frequency is 436 MHz in free band, communication speed is 9600 baud. There are four antennas convoluted in construction of probe, when reaching orbit, locking wires burn off and antennas will be protruded.

1.3.9 On-board computer

On-board computer is primarily operating other boards, synchronizing their requirements and measured data. It determines priority of the individual measurements and it switches between them. It also drives the power supply, except the situation of dangerously low value of voltage (see 1.3.2). Other important task is that OBC communicates with Earth's station.

1.3.10 FIPEX

For QB50 project are prescribed three sets of sensors for thermosphere research. It was possible to choose one of these sets - Ion-Neutral Mass Spectrometer (INMS), Flux-Φ-Probe Experiment (FIPEX) and multi-Needle Langmuir Probe (m-NLP). Each of them is accompanied by thermosensors. VZLUSat-1 has Flux-Φ-Probe Experiment (FIPEX) on board. This experiment studies behaviour of atomic oxygene in lower thermoshere. This element is dominant type in the incriminated region and its measurement is crucial in the correlation and validation of atmospheric models. Moreover, erosion of spacecraft surfaces due to the interaction with atomic oxygen is a serious concern and merits in-situ study in its own right. The measurement is based on solid oxide electrolyte micro-sensors. [5]

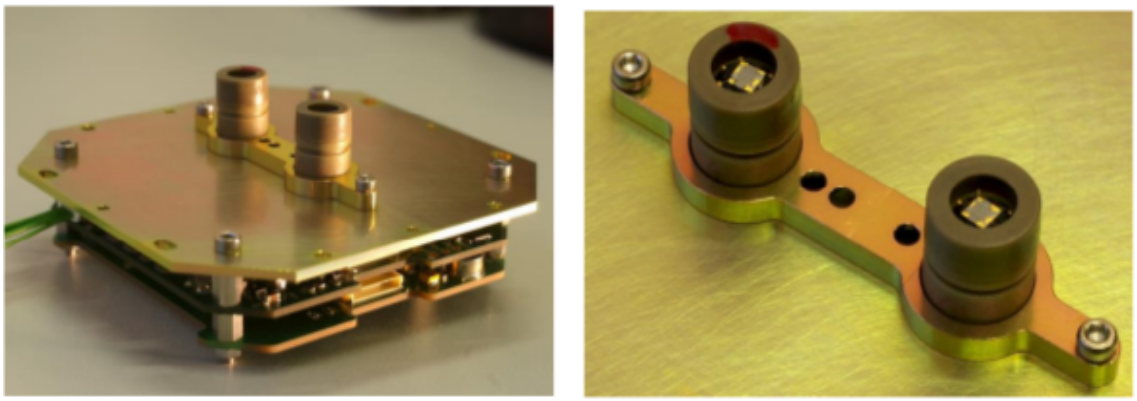

(a) FIPEX - board

(b) FIPEX - detail of the sensors

Fig. 1.5: Fipex [5]

2 Radiation environment on the Earth's orbit

In this chapter will be briefly described the operation conditions of VZLUSat-1. Magnetic and radiation environment of the Earth's surroundings is very complex and there are many factors which have to be considered. Because our task is to study radiation influence, especially on semiconductor parts, we have to know which sources of radiation are there and how the satellites and other orbital devices are protected from it.

2.1 Radiation environment and magnetosphere

Spatial distribution of the radiation environment surrounding the Earth is tightly connected with interactions between charged particles and planet's magnetic field. This field is not homogeneous. Its axis does not correspond with the axis of the Earth, they are about 520 kilometres misaligned from each other.

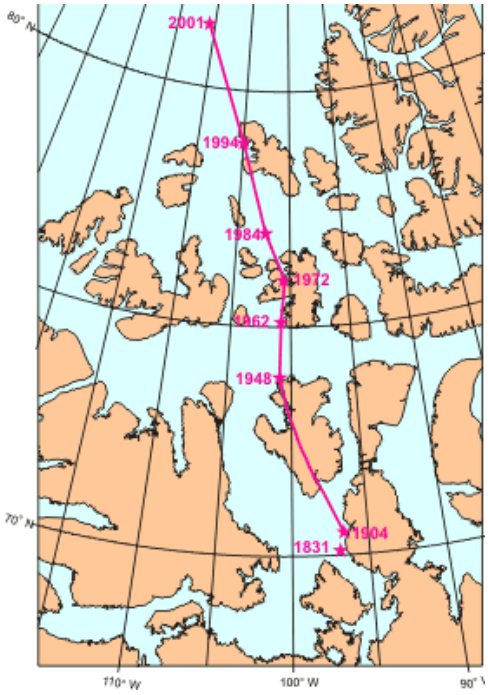

Fig. 2.1: Magnetic field travelling during the time [6]

The magnetic field axis is moving much faster as well, measurements show that it has moved for more than 10° latitude in last two hundreds years. Compared to this, Earth's axis rotates and one circle takes approximately 25 000 years. The magnetic field can switch too. Periods of changed polarity are called chrons, they last 450 000 years on average and during this change the strength of the magnetic fields drops under 10% of its present strength. When changes, magnetic field losses character of a dipole, the are several poles and field lines are not homogeneous. [7]

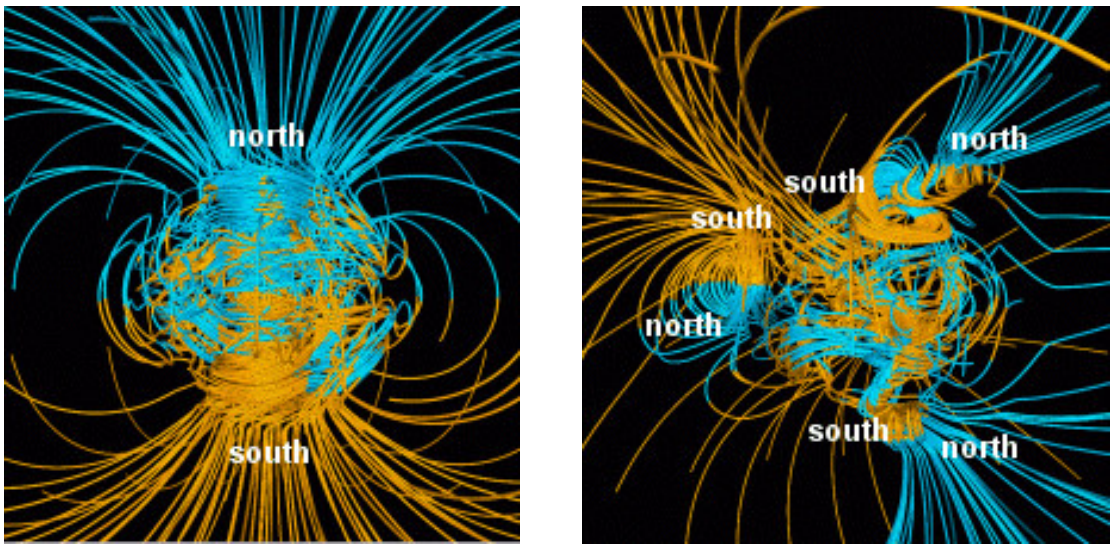

(a) Between reversals (b) During a reversal

Fig. 2.2: Reversal of magnetic field [6]

The shape of the magnetic field is drop-like. It is approximately bipolar at low altitude, but at high altitude it becomes highly affected by the solar wind and forms a geomagnetic tail behind the planet. This phenomenon is caused by the velocity of charged particles. Each point within the magnetic field has a minimum magnetic rigidity which the particle needs to hit this point. Particles below this level will be deflected. This minimum, called the cut off value, falls to zero at the edges of magnetosphere and at magnetic poles.

A satellite in Earth's orbit is protected against the cosmic rays, but the quality of this protection depends on the altitude and orientation, so we can say that the ones on geostationary and polar orbits are virtually without protection. Geostationary satellites must carry sufficient shielding if their orbit crosses the belts. It is one of the reasons why space stations stay relatively low orbit (International Space Station (ISS) maintains orbit about 400 km, Chinese Tchien-kung about 370 km, Mir oscillated between 296 km and 421 km), because astronauts cannot be exposed to the cosmic rays for a long time. [8–10] Another example of a sensitive device is

Hubble's telescope, which shuts down when it passes Van Allens belts. On the poles, there are regions called cusps, where the magnetosheath plasma has direct access to the ionosphere. Charged particles coming through have a contact with atmosphere in auroral oval, situated around 70° magnetic latitude. They excite atoms in the atmosphere, creating auroras. Most visible is green colour of Oxygen, 70 – 100 km altitude above the surface. Auroral oval also radiates in UV spectrum, this band is 1° – 5° wide and it has been documented from orbit.

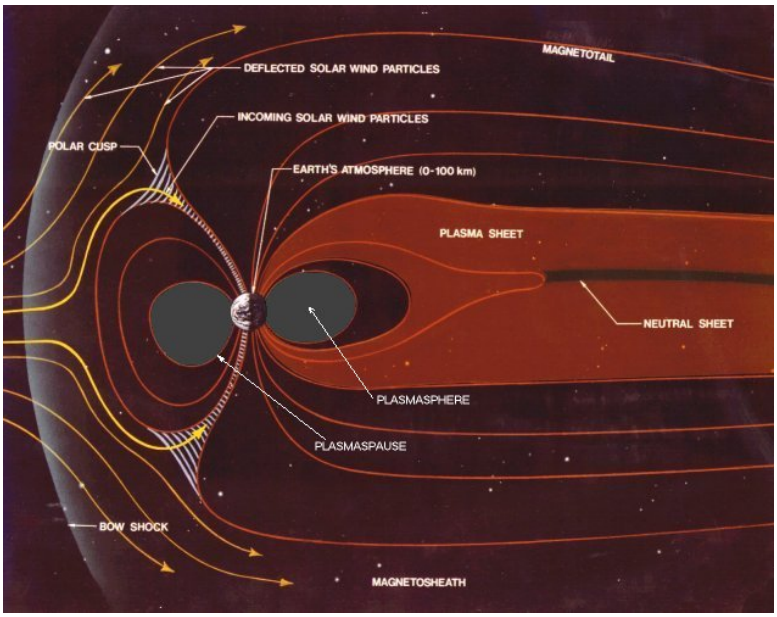

Fig. 2.3: Magnetosphere of the Earth - visible cusps and reconnecting field lines [11]

Sources of charged particles, mostly electrons and protons, are different. The most significant one is the solar wind. It strongly depends on the solar activity cycle. Its duration is approximately 11 years and reflects the changing frequency of solar flares and spots. The influence of solar wind is described by Disturbance Storm Time (DST) index. When charged particles arrive to the Earth, ring current increases. Because ring current produces a magnetic field in opposition to the planet's magnetic field, stronger current inflicts a decrease of protection against particles.

Significant fluxes of electrons are also supplied from Jupiter. The strongest emission is related to current system between Jupiter and Io. Streams of ions and high-energy electrons flow from Jupiter and interacts with our magnetosphere in the way similar to solar wind.

Magnetic field catches charged particles, which creates toroidal radiation belts known as Van Allen's. Their altitude extends from 1 000 to 60 000 km above the Earth's surface. We recognise two belts, but probes' missions into the Van Allens belts found out that it is probably possible to form the third one in the middle, which has only short duration and contains high-energy electrons.

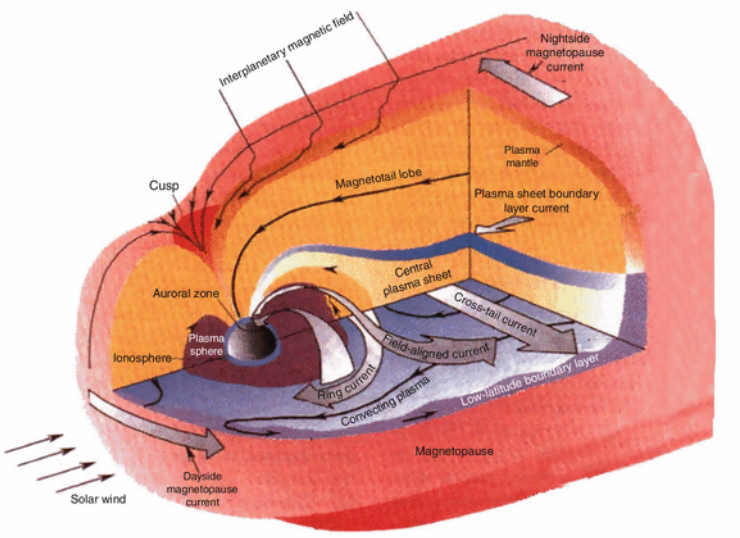

Fig. 2.4: Magnetosphere of the Earth - with visible currents [12]

Energy of particles is up to 7 MeV for electrons and several hundreds MeV for protons. Also the distribution varies; most energetic electrons are located in the farthest zone, most energetic protons at lower attitudes.

Electron environment is structured with two flux maxima, creating outer and inner electron zone. The outer zone approaches the Earth at high magnetic latitudes (60° – 70°), in regions where aurora phenomenon is typical. It is very dynamic, its cycles indicate a close link with solar flares and probably Jupiter's activity as well. Proton environment is simpler, it has only one flux maximum in the inner zone. [7]

2.2 Secondary radiation

When a real spacecraft is constructed, there is other complication accompanying the natural radiation. It is the secondary radiation generated by the interaction between spacecraft material and electrons, so called Bremsstrahlung X-Rays. There are secondary protons and neutrons generated by high-energy protons as well. These do not have such a high level of energy to degrade materials, but they can affect measurements and interfere with satellite's operation.

During the mission, the whole body of the Cube will emit this secondary radiation. Because XRB diodes, our sensors, are close to the rest of device and this radiation will impact on them from behind and could interfere with the desired signal from free space, it was necessary to solve shielding from this radiation. As a solution, 1 mm thick Tungsten plate was placed right on the XRB board and on its sides. [7]

2.3 Artificial radiation

During the Cold war many experiments were conducted to explore the possibilities that the satellites could be exposed to the nuclear weapons attacks in the space. This case is specific, because such an intense, transient pulse of natural origin is occurred by only one particle, but nuclear weapon emits short, but strong pulses of gamma rays and neutron and electromagnetic pulses which can last for milliseconds. It is important to know the dose-rate of transient effect and total dose which a component can absorb undamaged. Logical gates can switch logical states when exposed to high enough dose. A bistable circuit can stay in the wrong state. Bigger gates are generally less susceptible, because their mass simply contains more particles, which can be damaged before these disorders affect functionality of the device. [7]

2.4 The response to radiation

This chapter describes two main types of degradation processes in materials exposed to radiation dose, atomic displacement and ionisation. The dose can be specified as rads per second, that means average energy absorbed per mass unit and time. This method is especially suitable for high-energy electrons and photons. While passing through matter, these particles lose their energy on interaction with atoms of matter or scattering. There are also mentioned two effects which are bonded with energy transfer between particle and semiconducting materials, like Germanium and Silicone - the photoelectric effect and Compton scattering. [7]

2.4.1 Atomic displacement

A part of the energy of passing particles transforms into momentum of atoms of the absorber. When the energy is sufficient, an atom can be removed and leave a defect or vacancy. This atom then moves and can take place in another vacancy, or can come into an interstitial position in the lattice. Vacancies can move or make groups with another vacancies, they also can combine with impurity atoms. Vacancies can be active in semiconductors, but not the interstitial atoms.

$$I_\tau - I_{\tau_0} = K_\tau \Phi \tag{2.1}$$

In this formula, τ and τ_0 represents values of minority carriers lifetime before and after irradiation, K_τ is minority carrier lifetime damage constant. Φ stands for electron flux. Reference is often 1 MeV electron irradiation, other particles are compared to it. Because of low weight of electron, for example proton with the same kinetic energy will cause thousands more displacements.

For conductors, this type of degradation is not significant in space. Compared to, for example, reactor technologies, doses are too small to lead to serious changes in conductivity. Worse situation is with semiconductors, where displacement effects are long-lived and reduce mobility and lifetime of carriers. Most sensitive parts are bipolar transistors, which are nowadays generally rarely used, solar cells and silicon-controlled rectifiers. All of them require long lifetime of minority carriers. Also high electron mobility transistors are quite sensitive.

In optical materials, colour centres as mentioned in Fig. 2.6 are produced. The term colour centres includes all point lattice defects that absorb light in an area where the crystal itself would not absorb. Typically, it happens in inorganic crystals and glasses. In case it was produced by exposing to an ionising radiation, this colour centre is called induced colour centre. When there are another products of irradiation, like electrons and holes, these particles can get trapped in crystal defects and cause the appearance of new band in the spectrum and also a change in the colour. They can also cause chain reaction, produce new defects around the first, small centre, such as interstitial ions and vacancies generation. [13]

In general, dielectrics do not have problems with displacement of nuclei, capacitance and leakage current are not affected and more serious issue for them is ionisation. The review table 2.1 below shows a list of VZLUSat-1 components. XX stands for primary failure mode, X for secondary failure mode. [7]

Tab. 2.1: Atomic displacement effects in semiconductors [7]

Device	Carrier life-time reduction	Carr. removal by trapping	Mobility decrease	Slow emptying of traps
MOS/MIS FET		XX		
Rectifying diodes	XX	X		
Schottky diodes	XX	X		
Solar cells	XX	X		
Zener, IMPATT	X	XX		
Hall effect dev.		X	XX	
Photoconductive photosensors			X	X
Transferred el. dev.		X		XX
Junction FETs		XX	X	
Mech. transducers		XX	X	

2.4.2 Ionisation

When atomic displacement means transfer of momentum, ionisation is a process of valence band electron excitation to the conduction band. These electrons are more mobile in an electric field, in semiconductors they form and electron-hole pair, creating spurious photo-currents. These can be registered as background noise in sensitive circuits. Any solid material, even insulator, is more conductive than in normal conditions. The creation of positive charge carrying holes causes serious degradation in components consisting of oxide layers, such as MOSFETs. Energy, needed for creating a pair, is relatively small, about 18 eV for SiO_2. The magnitude of this effect depends on the dose at time, rather than on total dose. Expected dosages in orbit are too small to cause latch-up or logic upset in transistors, especially when are not used extremely small versions of parts.

In dielectrics, scale of harmful effects is wider due to their greater variety compared to the semiconductors. Also the gap between valence and conduction bands is wider, so variety of trapping levels and excitations is possible and polarisation effects can be long-lived. The effect of ionisation can be accompanied by rearrangement of atomic bonds and chemical decomposition, but it is mainly a problem in organic dielectrics.

In table Tab. 2.2 the X symbol represents the degree of sensitivity of chosen devices. However, there is not disregarded the magnitude, so it is possible that any devices, which are affected and crossed in the same column, can suffer in fact worse damage than another with same sphere of negative effects. [7]

Tab. 2.2: Ionisation in dielectric - Long-lived effects [7]

Device	Retrapped locally	Charge transport	Bonding changes only	Decomposition
Special MIS systems		X		
Storage photosensors		X		X
Bipolar, MOS, CCD		X		
Capacitor insulators		X	X	X
Thermoplastic memories			X	X
Lenses, filtres	X		X	
Refractory layers			X	X
Pyroelectric detectors				X
Electroluminiscent phosphors	X	X	X	

2.4.3 The photoelectric effect

In a photoelectric encounter, the entire photon energy is absorbed by an atomic electron. The kinetic energy of this electron increases, it moves to higher orbital. We recognise two kinds of this effect, one is, when excited electron remains inside the irradiated material, called inside photoelectric effect. The electrons are rising the conductivity of the material. They can be released from the material completely as well, then the effect is so called outside photoelectric effect.

$$h_\nu = h_{\nu 0} + E_{max} \tag{2.2}$$

Where $h_{\nu 0}$ means minimal energy needed to release an electron and E_{max} stands for maximal energy of released electron. h_ν is the energy of impacting photon.

For the photoelectric effect, a monoenergetic Gamma ray gives rise to a monoenergetic peak in the charge distribution. This peak corresponds to the incident photon energy.

2.4.4 Compton scattering

When a photon is scattered by an electron, a part of energy of this photon is transfigured into energy of the electron. The amount of energy the photon lost depends on the angle of scattering. When the energy of photon changes, changes also its wavelength. This phenomenon is called Compton shift. This effect was one of proves supporting the theory, it is necessary to consider light as particle and as radiation in the same time. Energy of a photon after the process of scattering can be evaluated from

$$E_s = \frac{E}{1 + \frac{E(1-cos\Theta)}{511\,000}} \tag{2.3}$$

where 511 000 is an annihilation energy of an electron in eV, according to formula (2.4), Θ is an angle, to which the photon diverts after the Compton scattering, E is the original energy of photon and E_s is the energy after Compton scattering. This effect was one of proves to support theory of dualism.

$$E = m \cdot c^2 \tag{2.4}$$

where E is total energy of particle, m weight of an electron and c the speed of light.

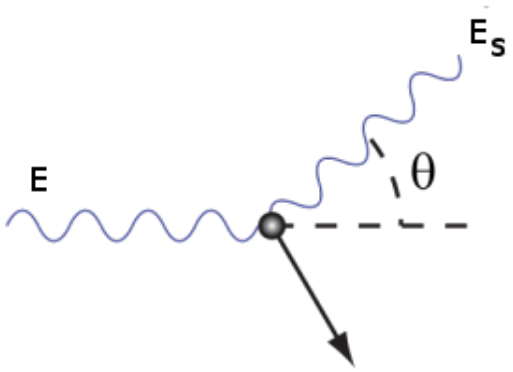

Fig. 2.5: Compton scattering

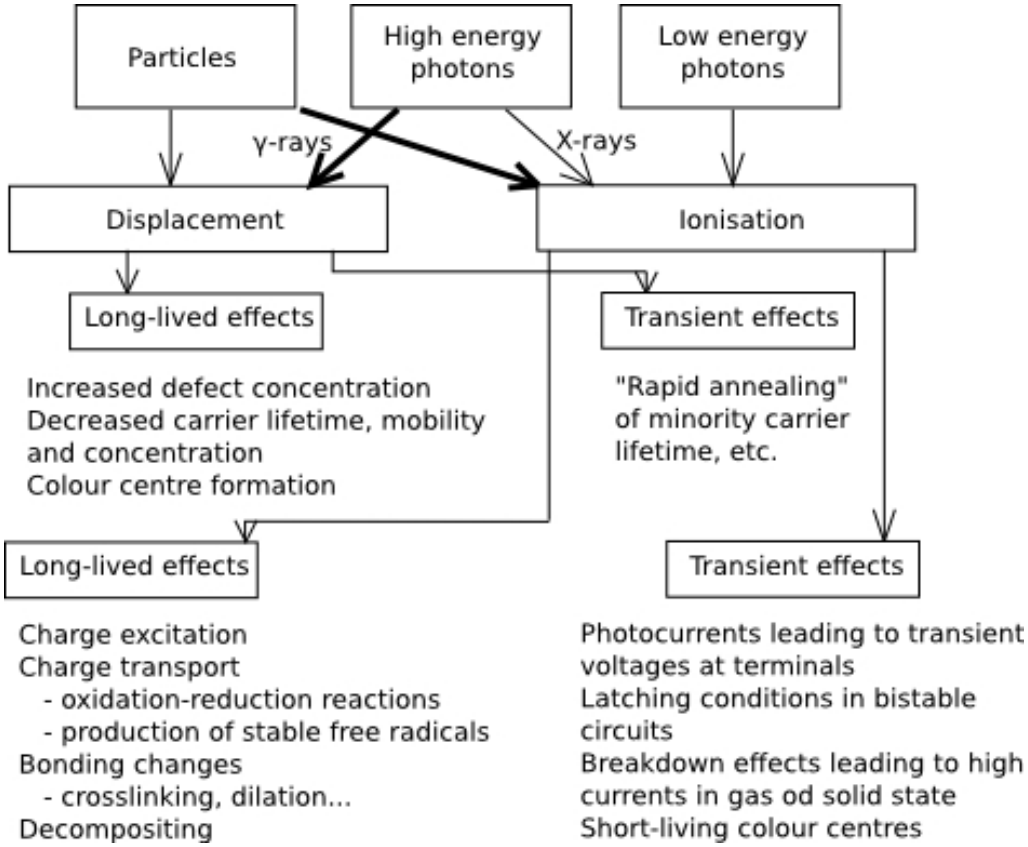

Fig. 2.6: A summary of radiation induced degradation effects [7]

3 Radiation testing

The reaction and sensitivity of semiconductor parts to radiation varies and is impossible to predict. Therefore irradiation tests must be an integral part of the development of devices. The simulation of space radiation effects is difficult to achieve and the results are often different than expected. The incident space radiation is a complex mixture of different particles and rays, which can further change while passing through spacecraft. This complex dose will be delivered over a long period of time, often several years. Basic radiation sources and used methods of measurement are discussed in this chapter.

3.1 Radiation - spectre and sources

Electromagnetic spectrum is the range of frequencies or wavelengths of electromagnetic radiation. It ranges from extremely long frequencies of units of Hz over wavelengths used for communication and visible light to short, penetrating radiation like Gamma rays. Wavelength, frequency and energy of a photon can be calculated by using following equations

$$\lambda = \frac{c}{f} \tag{3.1}$$

$$f = \frac{E}{h} \tag{3.2}$$

$$E = \frac{h \cdot c}{\lambda} \tag{3.3}$$

where c = 299792458 $\mathrm{m{\cdot}s^{-1}}$ is the speed of light in vacuum, λ is the wavelength, f the frequency of the photon, E energy of the photon and h = 4.135667·10^{-15} J·s is Planck's constant.

Basic distribution of the spectrum is illustrated in Fig. 3.2: radio waves, according to ITU standard, are waves longer than 15 cm. In astronomy, in radio spectrum radiates objects like black holes spurts or dust and molecular clouds. Shorter are microwaves with lengths from 0.4 mm to 15 cm, that means 20 GHz to 750 GHz. In space research we can find relict radiation after the Big bang, from stars during

their birth or, from artificial sources, like GPS satellites. Next follows infra-red, with lengths from 0.75 µm to 400 µm. This part of the spectrum is used for distance research of the Earth, interplanetary mass, red dwarfs or exoplanets. IR comes through the atmosphere only partially, shorter waves are more successful. Frequency of visible light can be measured in units of THz, this corresponds to wave lengths 380 - 750 nm. We can observe typical colour lines of elements as Hydrogen or Oxygen are. Ultraviolet spectrum, from 10 nm to 390 nm, is produced by stars, typically by young, hot stars, auroras novas and supernovas. Most interesting for this work are the three shortest types of radiation. These are soft X-Rays, with energy around 6.9 keV and length 0.1 to 10 nm, hard X-Rays between 0.01 and 0.1 nm and Gamma rays, which is simply shorter than 10 pm. In space, sources of these penetrating rays are high energetic processes around accretion disks of black holes, pulsars or white dwarfs, and also during the process of magnetic reconnection of field lines in stars' atmospheres.

Frequency						
<2 GHz	2 - 750 GHz	0.75 - 400 THz	400 - 789 THz	0.79 - 30 PHz	30 - 300 PHz	3 - 30 EHz
Wavelength						
>15cm	0.4 - 15 cm	0.75 - 400 µm	380 - 750 nm	10 - 380 nm	0.1 - 10 nm	10 - 100 pm

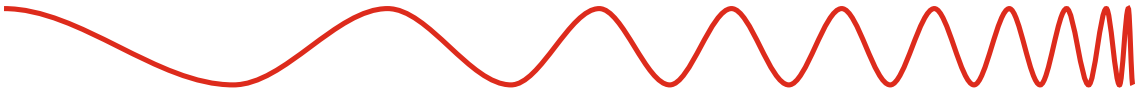

Fig. 3.1: Electromagnetic spectrum - frequencies and wavelenths

Wavelength distribution can slightly vary across different publications, because rays are divided according to their frequency as well as to their origin. That means, any kinds of hard X-Rays can have wavelengths shorter than is classified for Gamma, but because these rays do not appear as a result of atomic nucleus decaying but have their origin in electron orbitals, they are still called X-Rays. The behaviour of electromagnetic radiation depends on its wavelength and when the interaction with single atoms and particles is studied, also on the amount of energy it carries. In this thesis was used the classification of radiation spectrum as it is typical for astronomic purposes. [14]

3.1.1 Gamma rays

Gamma rays are high - energy photons of very short wave length. It is the most penetrating kind of radiation, it is ionizing and biologically hazardous, damaging DNA information. Gamma rays are emitted by the decay of atomic nucleus, usually together with alpha and beta radiation. Usually, this kind of radiation is characterised by wavelength under 10^{-11} m (0.1 Å).

Commonly used sources for simulation are active Cobalt-60, Cesium-197 and Americium-241. Cobalt-60 is produced from inactive Co-59 by heavy neutron irradiation. The process of decay can be divided into two phases. In the first, Co-60 decays to excited Ni-60, an electron, a neutrino and 1.17 MeV gamma ray. In the second phase, Ni returns to the ground state and emits 1.33 MeV. Half-life of Cobalt-60 is 5.27 years.

$$^{60}_{27}Co \rightarrow ^{60}_{28}Ni^{*} + e^{-} + \bar{\nu_e} + \gamma + 1.17MeV \tag{3.4}$$

$$^{60}_{28}Ni^{*} \rightarrow ^{60}_{28}Ni + \gamma + 1.33MeV \tag{3.5}$$

Americium isotope is artificially produced as a decay product of plutonium-241. Decaying Americium-241 to Neptunium Np-237 is an Alpha decay, but in addition, it radiates small amounts of Gamma rays as a by-product. These rays are 1.33 MeV and the emission spectrum is complex. Half-life of Am is 432.2 years, the final product of decay is Bismuth-209.

$$^{241}Am \rightarrow ^{237}Np + \gamma + 1.33MeV \tag{3.6}$$

Cesium Cs-137 with half-life of 30.17 years is produced when neutron is absorbed by plutonium and uranium and undergoes fission. It decays in two phases again, by Beta emission to metastable Barium-137 and by Gamma to the stable ground state of Ba-137. The energy of radiated rays is 662 keV.

$$^{137}_{55}Cs \rightarrow ^{137}_{56}Ba^{*} + e^{-} + \bar{\nu_e} \rightarrow ^{137}_{56}Ba + \gamma + 662keV \tag{3.7}$$

3.1.2 X-Rays

X-Rays simulate the cosmic environment by inducing ionisation, similar to gamma-ray effects. Compared to Gamma, X-rays have different origin and wavelength. As it has been mentioned before, Gamma-ray is generated when a nucleus decays, but X-rays have their origin in electron orbitals and typical wavelength ranging from 0.01 to 10 nm. As mentioned above, X-rays are further divided to hard rays with energies above 5-10 keV and soft rays with lower energy. Typical source of X-Rays is bremsstrahlung. It is a kind of electromagnetic radiation produced by deceleration of charged particle deflected by another one. The moving particle loses its kinetic energy, which converts into a photon. Higher frequencies are associated with increasing of the energy of accelerated particles. Compared to radiation from decaying, bremsstrahlung has continuous spectrum.

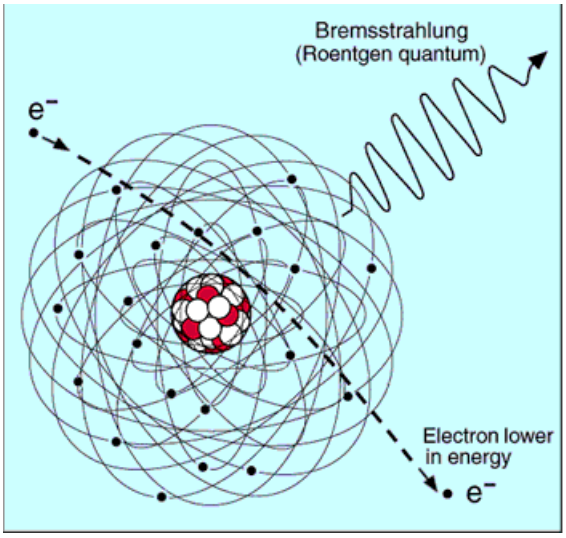

Fig. 3.2: Process of X-Ray emitting [15]

4 Radiation detectors

The material suitable for radiation detection must be grown in high purity and constant quality. They are also need to be quite big, it is the reason why CdTe detectors were not used for a long time, despite of their other properties. Used materials are silicone, germanium, which has higher atomic number Z and due to it much higher probability of interaction with radiation, and other materials, like CdTe or HgI_2. On VZLUSat-1, there are three XRB diodes and one CdTe detector, so they will be mentioned in more details.

4.1 XRB diodes

Diodes mounted on the XRB board are based on silicone and can detect energies ranging from 5 keV to 20 keV. Despite the excellent charge transport properties and energy resolution of silicone, it has low stopping power for high energy photons and this is limiting for their application to Gamma and hard X-Rays detection. Effectiveness of higher energy radiation detection can be increased by inserting higher voltage. Unfortunately, this step has a negative side effect – dark current rise. Dark current is a state of a photodiode, in which it has small electric current even when there are no particles entering the device. It is present in every diode and it's impossible to get rid of it, because it has physical cause in random generation of electrons and holes within the depletion region of device. The rate of generation depends on the temperature and biasing proportionally and it is related with crystallographic structure and defects of silicone. The crystallographic grid is moving and sometimes an electron gets enough energy to leave its orbital place. These free electrons and holes respective to them are then moving through the depletion region. With higher temperature and biasing voltage, the probability of electron – hole generation rises. It produces a shot noise and in the worst case, when we use strongest possible power supply and the satellite is on the light side, small useful signals may drown in the noise. Moving of the edge depending on temperature is also shown in figures made during practical part of my diploma thesis. In praxis on the Earth, devices are cooled so the effect of temperature can be eliminated or at least reduced.

In space, it is impossible to use conventional heat-sinks; the only way of cooling is radiative heat transfer.

4.2 CdTe detectors

Cadmium-Telluride seems to be promising semiconductor material for detecting hard X-Rays and Gamma rays. Compared to silicone, both materials have high atomic number, $Z_{Cd} = 48$, $Z_{Te} = 52$, which gives them high quantum efficiency suitable for a sensor operating typically in the 10 - 500 keV range. They also have wider band-gap and can operate at room-temperature, so the problem of cooling is irrelevant in this case. The potential of CdTe detectors was regarded in the 70', but their use was a problem for the lack of stability. In the 90', Traveling Heater Method was used to grow large, pure CdTe crystals with good charge transport properties.

VZLUSat-1 has a CdTe detector located on the Measure board. It has bias voltage 200 V, while XRB diodes need only 60 V. The rest of schematic of analogue amplifiers is analogous to the one used on XRB board, according to scheme Fig. 6.4. It will be able to measure energies up to 200 keV. The design of grounded cover around the detector itself is noteworthy. Measure board carries several different voltage power sources, as mentioned earlier, CdTe detector needs 200 V, XRB diodes need 50 V. The board also includes CPLD and microcontroller unit, which need 3.3 V and 1.8 V. Other devices use -2.5 V, -3.3 V, 4.5 V, 5 V, 3 V and 2.5 V further. All these parts are significant sources of unwanted noise, especially digital signals travelling between CPLD and microcontroller. Grounded housing creates a protected zone for sensitive signal from CdTe detector, before it gets amplified enough. [16]

5 Problematic of amplifiers

An amplifier is an electronic device which amplify input signal using especially feedback. The amplifier takes input low amplitude of signal and amplify it, in depending on ratio of feedback, into the usually higher output amplitude. We differentiate four basic types of amplifiers. Voltage, which is most common, with low output and high input impedance. Current, where are these impedances reversed. The second opposite pair is a transconductance amplifier, which changes output current depending on input voltage and transimpedance changing output voltage in dependence on the input current. Their output can be linear or non-linear. First way how to amplify a signal was using vacuum tube, which was invented in the beginning of 20^{th} century. In 1954 was made the first transistor. Because of its size and severity, they spread fast and vacuum tubes were pushed out. Nowadays vacuum tubes are used only for special occasions, as are high-end top quality professional audio aparatures or as power amplifier in a big transmitter. Different types of vacuum tubes are used as a source of radiation, microwaves or X-rays.

5.1 Essential properties of amplifiers

Every application of amplifiers needs different access. Amplifiers have many different properties and suitability of their combination is directly related to the purpose of use. Nice example are audio amplifiers - of course the gain is necessity, but more important is to have exactly the same shape of signal at the output, even at the expense of amplification cardinality.

In this case, I can mention three main properties, which were emphasized. Noise, because awaited signals are very weak and noising amplifier could destroy it. This parameter was most essential, even at the expense of power requirements.

The next important parameter is slew rate at unity gain. The faster slew rate is, the higher frequencies can the amplifier transfer. Definition of instant speed is a tangent line to the signal shape, as seen in Fig. 5.1. When slew rate is too low and below this tangent, a part of signal is lost and its shape gets deformed. When the slew-rate is too high compared to the frequency of transferred signal, it can cause noise on higher harmonic frequencies, so it is good to use values from the adequate

range.

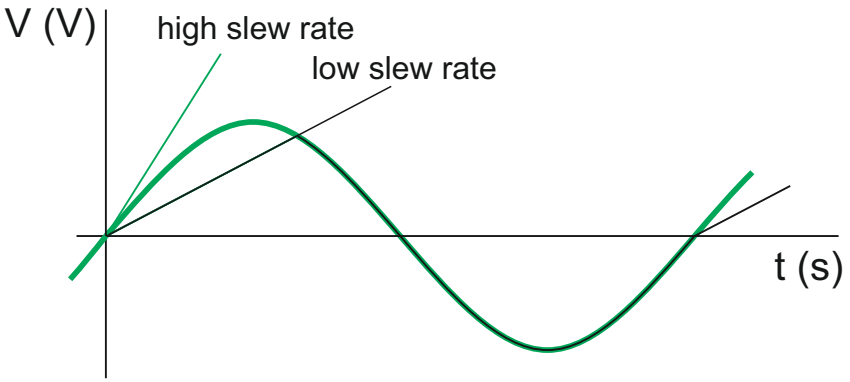

Fig. 5.1: Slew-rate influence on the shape of signal

Another important parameter is power consumption. Our satellite has a limitation 2 W for the whole device, so it was necessary to use parts with lower consumption, although parts with better other parameters could be bought.

5.2 Aplifier for XRB diodes

Now take a look at our amplifier. In the beginning, there is XRB diode. It is connected to coupling capacitor, which serves to separate DC Biasing voltage 60 V is led from Measure board. There is RC filter, which prevents peaks and noise in general incoming from that board. Transistor T1 is manually selected and tested low-noise FET. Operation amplifier, which is the next part in the cascade, has not an output of inner structure. That means, we cannot adapt inside asymetry. And just this problem solves selected FET, which improves parameters. On its gate is very small current, about fA. OpAmp U100 serves as charge preamplifier. Amplifying is determined by 1 GΩ resistor in feedback, paralel with 1.1 pF (measured, sold as 1 pF) capacitor. Recalculation of 1 MeV energy photon on input for 1 pF capacitor should match 44 mV for silicone. This value depends on the amount of energy needed to generate a pair electron – hole. This energy of basic materials used as radiation sensors on CUBESat-1 is in Tab. 5.1 The gain of preamplifier is calculated according to formula

$$Q_P = \frac{E \cdot e}{\epsilon} \tag{5.1}$$

where E is energy of the incident radiation in eV, e is the charge of an electron and ϵ is an amount of energy needed to generate the conductive pair.

Tab. 5.1: Amount of energy needed to generate a pair electron - hole [17]

Detector	Energy ϵ (eV)
Silicon	3.62 to 3.71
Germanium	2.96
CdTe	4.43
CdZnTe	5.00

$$V_0 = \frac{Q_D}{C_f} \tag{5.2}$$

$$\tau_t = R_f \cdot C_f \tag{5.3}$$

where V_0 is the amplitude of the output voltage from preamplifier, Q_D is the charge released by the detector, τ a decay time constant and C_f and R_f are the feedback capacitor and resistor. The stability of preamplifier depends on the stability of C_f and the gain of preamplifier loop, which must be very high to neglect small changes.

The real value is a little different – we have to calculate not only with the capacity of capacitor, which really is 1.1 pF, but also with capacity of printed circuit, which is approximately about 0.05 pF and parasite capacity of 1 GΩ resistor. These three capacities are parallel, that means 1.25 pF. The gain with this capacity according to (5.1 - 5.3) is

$$\frac{V_0}{E} = \frac{1.6 \cdot 10^{-19}}{1.25 \cdot 10^{-12} \cdot 3.62} \doteq 3.54 \cdot 10^{-8} \frac{V}{eV} \tag{5.4}$$

Behind this amplifier are three other stages, shaping ones - one derivative and two integrating. This was made again due to requirements on noise. There could be also one derivative and only one integrating, but this solution would increase noise. Final shape is semi-Gaussian – raising edge is Gaussian, falling edge, created only by one derivation, is more gradual. Time constant is given by ratio of R and C elements according to (5.3)and is 2.2 µs and again, shorter time constant could lead to higher noise.

Capacitors on power supply of shaping stages serves as low-pass filters. There are pairs with lower and higher value, order nF and µF. Lower capacitance of capacitor is placed closer to incriminate OpAmp and filters higher frequencies, higher capacitance lower frequencies. Resistors on voltage input, like R112, prevent before

latches, separate signal from noise in supply and provides better stability of power supply. [17]

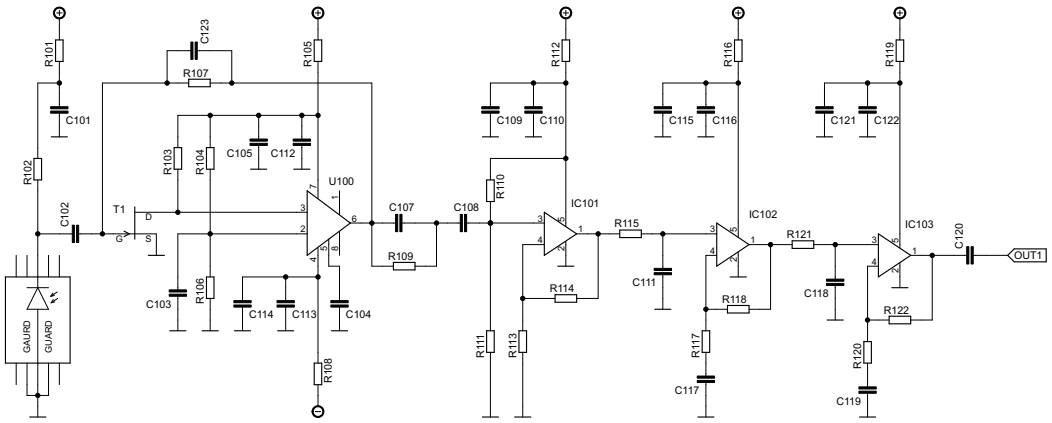

Fig. 5.2: One channel of low-noise preamplifier

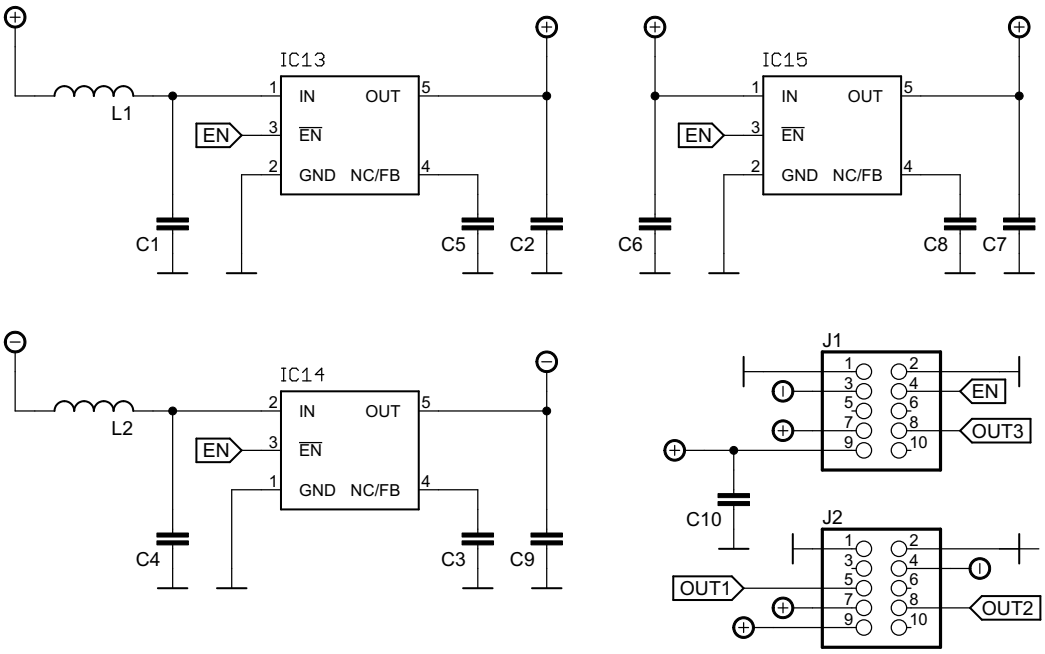

Fig. 5.3: Power supply for OpAmps situated on XRB board

6 Printed circuit board

When the schematic was accepted, I had to create a board, using all known principles of design. I got to the project after two years it was running, so at this time, there were another three versions of my board. None of them was fully functional. I took over the work and made my own design. As you can see in the schematic, there are three amplifying stages. The design seemed to be a simple task, but I found out early where were the problems and why all older versions weren't applicable. [18]

As mentioned before, VZLUSat-1 carries several tasks and room inside the satellite is limited. Due to it, XRB board, situated outside the body of probe and perpendicular to Measure board, has strictly prescribed dimensions and position. Originally a simple task is suddenly relatively complicated, because connectors J1 and J2 which connect both boards are situated almost in the middle of XRB board. Also placement of XRB diodes was fixed, they have to fit in windows in composite housing – situated in the middle too, but on the other side. That causes that amplifying stages can not be designed from the beginning to the end ideally, they must encircle the connectors. The beginning and the end of amplifying road is close, but output signal is several orders of magnitude higher; there is a danger of crosstalks between channels and also maybe between beginning and end of one channel too.

For space boards, only two layer boards are permissible. Four and more layers can keep humidity inside, which will evaporate in vacuum and cause damages of Printed Circuit Board (PCB). The same problem is with air bubbles, which would expand as well. Parts are placed only on one side, inside the probe. On the outside, there are three XRB diodes, facing the space.

There is standardized size of parts too, the smallest packages cannot be used in space. I knew that everything will be hand-soldered too. That means, I had to place over 150 parts onto one-sided 22 cm^2 board, with necessary spacing between signals, channels, power supply and mounts.

6.1 First version

I started my first version, with the same dimensions as the last version made by my predecessor. Also the orientation of diodes and all measures between connectors and board edges were strictly observed. You can see that this one has only three amplifying stages and connectors. In this phase, power supply was provided by Measure board, XRB board was really only an amplifier for desired signals from diodes. Between relatively high voltage, 60 V XRB bias, and split ground is wider space.

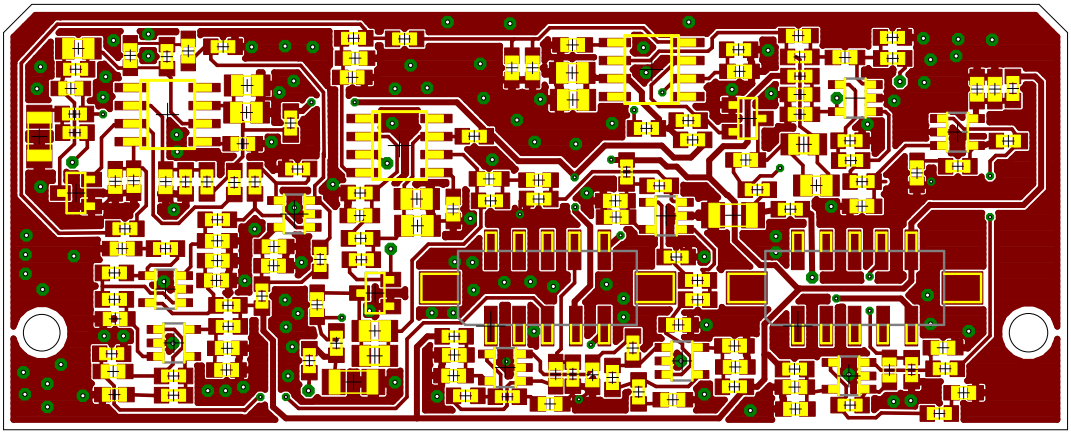

Fig. 6.1: Board - first version, top side

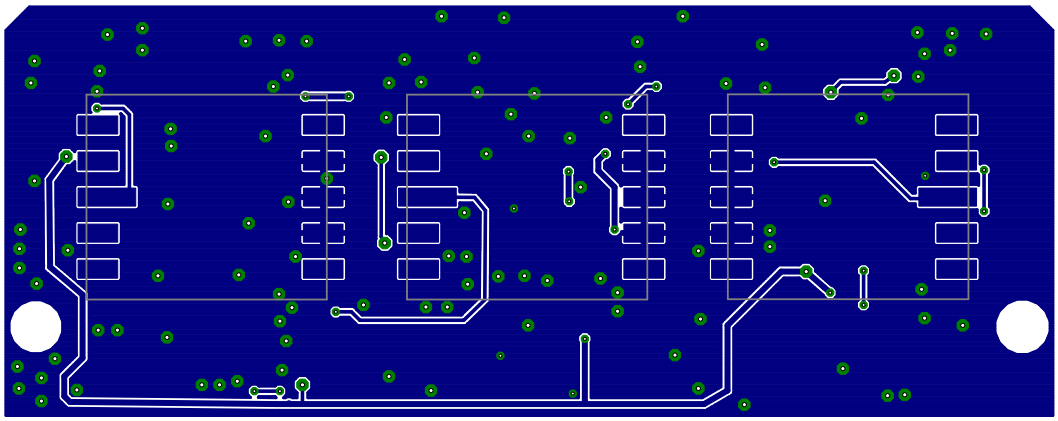

Fig. 6.2: Board - first version, bottom side

That serves to avoid leakage current, which is a small current constantly flowing to the ground. This current generates dissipation of energy and noise. Connectors are

the most vulnerable parts, so all the supplies were doubled. When one connector fails, the second one is able to supply diodes and at least one signal will come from XRB to Measure board. In this version we used tungsten shielding from both sides of the board, to protect parts against cosmic rays damages and to protect diodes against secondary radiation from behind, which could misinterpret signals. This embodiment protects diodes against the parts inside the Cube, as much as against secondary radiation from XRB board itself. Shielding was compact, easy to mount and to manufacture.

The board was manufactured, mounted and tested. First channel worked satisfyingly, noise level was about 9 keV. The second and the third had higher noise, the third channel was unusable. Although the board was grounded, with areas of spilled copper and high amount of vias, input signal from diodes was too weak and strong, amplified signal in the end of the second channel crosstalked with it.

6.2 Second version

My second version became more complex. Power supply for XRB board on Measure board was removed, I had to place three of them on my small board. They were placed between the second and the third channel and provide -2.5 V, +3.3 V and +4.5 V. Schematic of this power supply is in the picture Fig. 5.3. Measure board provides now only +5 V and XRB diodes bias +60 V. There will be less used pins on connectors, I got rid of doubling and supply path simplifies. Because noise levels on tested board were within parameters and we were in a hurry, I decided to preserve the first layout and only add new parts.

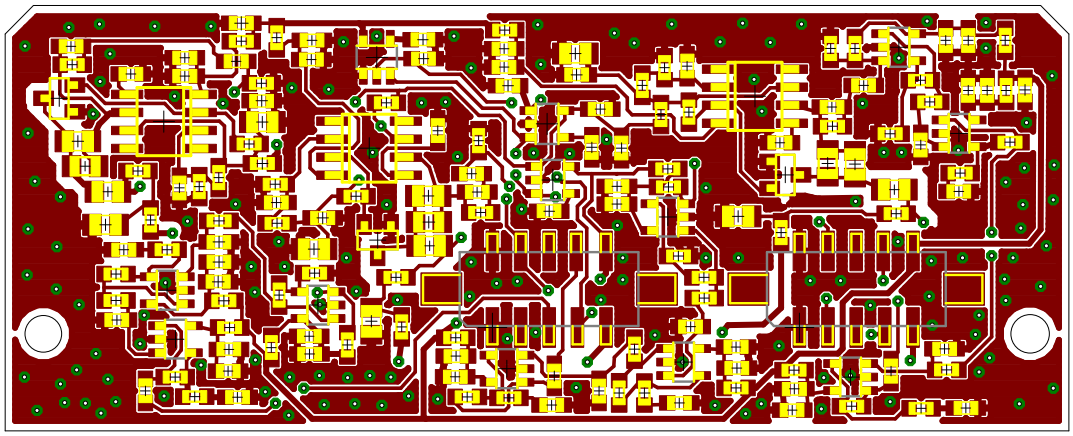

Fig. 6.3: Board - second version, top side

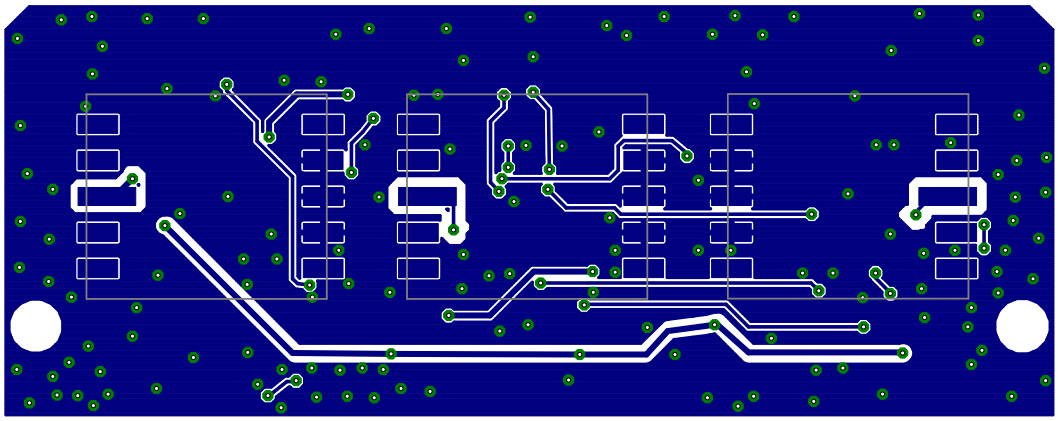

Fig. 6.4: Board - second version, bottom side

Measurement proved that this solution was not ideal, there still were small cross-talks between the second and third channel, especially compared to the first one, which had enough space and the best arrangement.

6.3 Third version

Due to unexpected complications in other tasks and measurements, deadlines were moved forward and former lack of time disappeared. So I got a chance to upgrade my board once again, this time with less stress and the possibility of using new information and experience from other versions. Schematics remained the same as in the second version, with power supply on board. Because of cross-talks risk, we were discussing the ways how to prevent them reliably. Here came an idea of a kind of electromagnetic walls between critical parts. In the picture of layout, Fig. 6.5, there are areas without soldering mask, where small pieces of metal will be mounted (Fig. 6.9). The height of these barriers is the same as the height of the tallest affected parts, that means 3 mm. I counted with thickness of tungsten housing and of course depth of connectors leading to Measure board, but 3 mm are enough. The housing, barriers and board will be bonded with ground, so high shielding effectiveness can be expected.

In this, probably last version, there are also vias, which will ground even the screws holding tungsten shield, Measure board and XRB board together. Electromagnetic waves will be led around the channel not only in plane, but the field will close from top and bottom too and the impact of cross-talks will be reduced. There is a separate chapter about measuring this effect. On the side with diodes, there are another unmasked fields, for shielding sheet protecting XRB diodes from behind. In case we would used Through Hole Technology (THT) diodes, we could use one

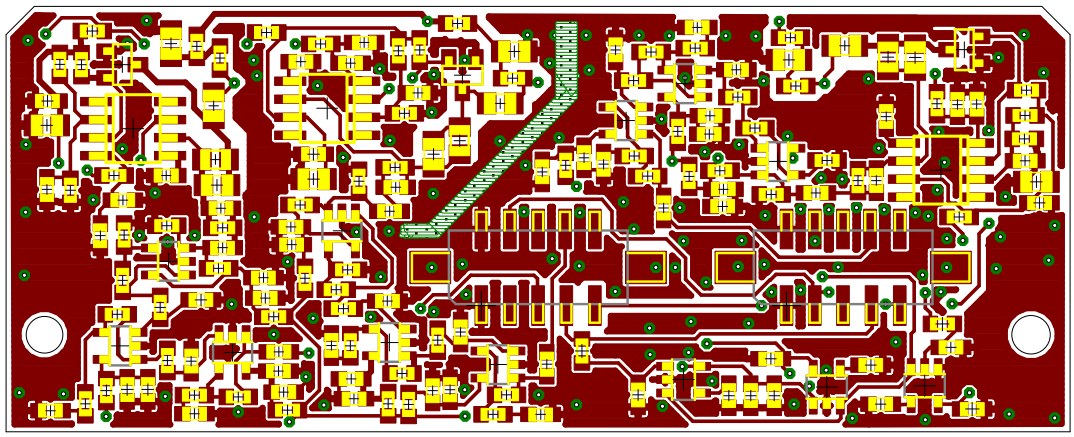

Fig. 6.5: Board - third version, top side

piece of tungsten with six holes for contacts, but because used diodes are Surface Montage Device (SMD) type, shielding is solved this way.

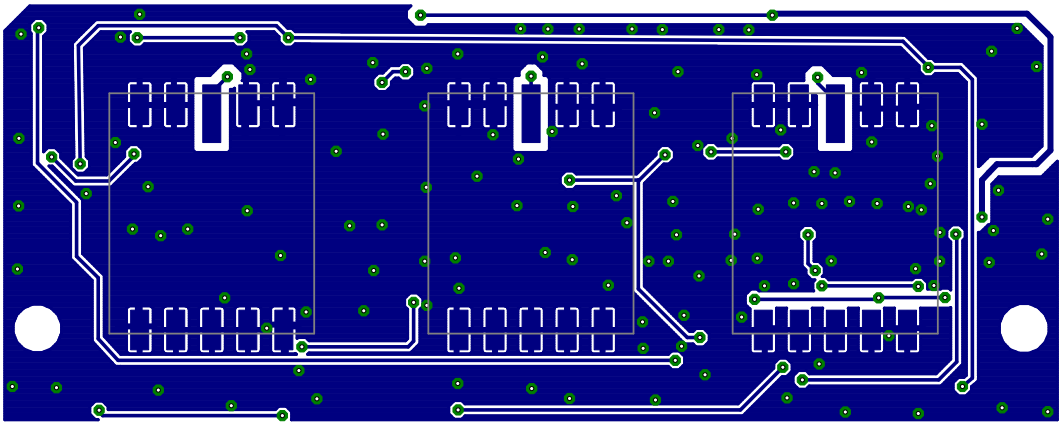

Fig. 6.6: Board - third version, bottom side

I was trying to arrange parts more logically, so the PIN diodes were rotated and channels are less curved. Power supply is moved and it creates a block under the connectors, newly there are ferit pearls, placed as close to connectors as possible. Unfortunately, there are still two strict places – the middle of PIN diode's active layer has to pass into the housing and connectors must fit into Measure board, so the second and third channel still have significantly less space and worse conditions. Although, above-mentioned measures should suffice. [18] In the pictures Fig. 6.8, Fig. 6.7 you can see mounted final version with Tungsten sheet on the backs of diodes and protective foil on the active layers. [19]

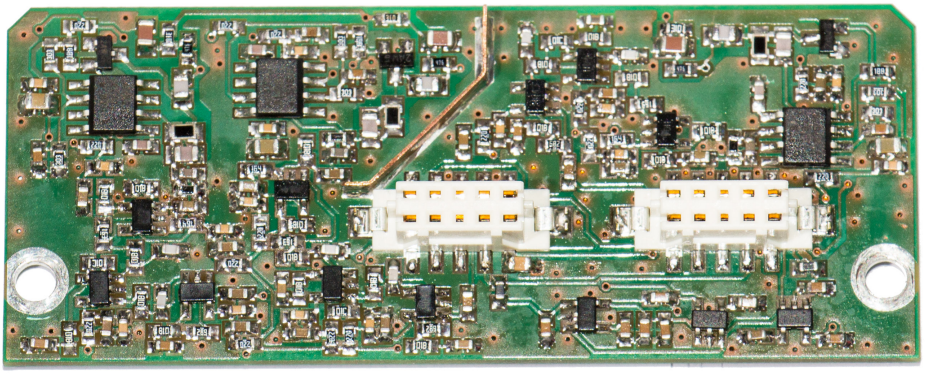

Fig. 6.7: Final version, top side

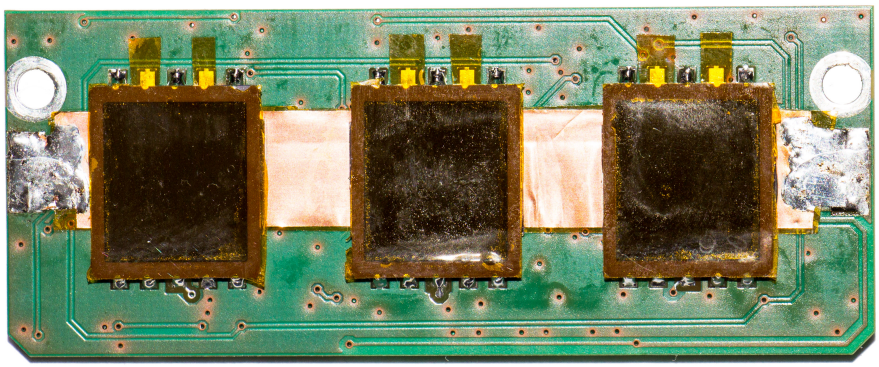

Fig. 6.8: Final version, bottom side

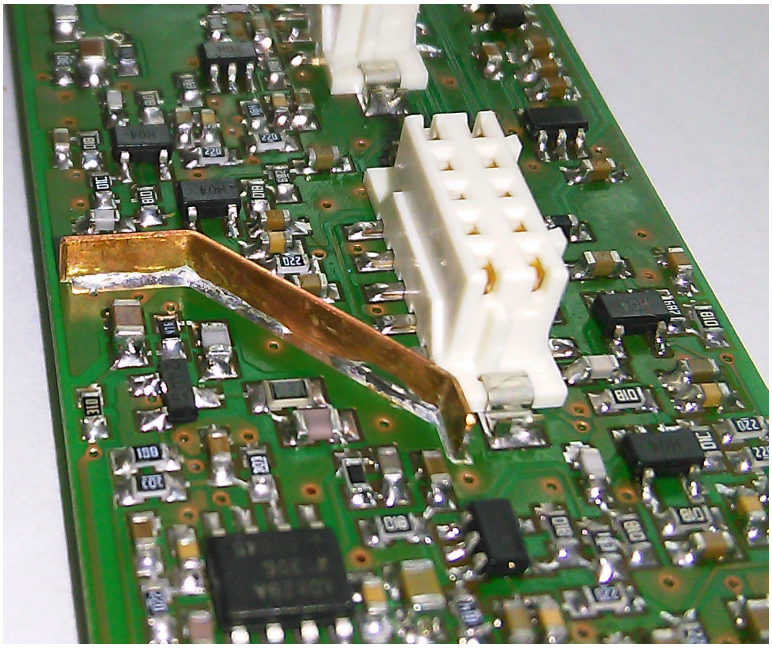

Fig. 6.9: Detail of Copper wall eliminating the cross-talks

7 Electromagnetic compatibility

Electromagnetic compatibility (EMC) is defined as an ability enabling a device to operate correctly in environment, where there are other sources of electromagnetic signals and also with its own function to not affect other devices impermissible. Importance of this discipline grows with increasing amounts of electronic devices, especially microprocessors and communication devices. The compatibility has different stages, depending on a degree of affliction. In case of independent space probe without operator, only the first three stages are possible-no affection or minor affection, without memorised data loss. When the interference fades out, functionality must be spontaneously restored in original range and quality. In the worst case, conditions can set it out of operation completely, but it still must restore. This situation can occur for example after a strong Sun flare.

In space, there is a specific situation. Our device is technically alone, the main problem may occur itself. Strongest sources of noise are digital processors and communication. In the next subsections I am going to describe elementary kinds of interferences.

7.1 Galvanic connection

This type of connection is also called common impedance and it forms between two or more electric blocks, which have common ground or power supply. That creates a current loop coming through shared impedance and appears as a noise voltage U_n. To eliminate the effect of galvanic connection, different kinds of separators can be applied. In this work there was neither space nor reason for devices as a separating transformer or optocouplers, but there are ferit pearls placed close to the connectors of the power supply. These pearls increase ground loop impedance and positive effect is high loss rate of ferromagnetic materials as well, which absorbs high-frequency noise.

7.2 Capacitive connection

Capacitive connection exists due to parasitic capacitance between conductors or parts of circuit or device's construction. Problem with this connection is bigger when permittivity of isolation is higher, as well as with fastness of time differences of signals. In general, it is better to work with minimal speed of signals (slew rate) as is necessary for the function. Higher speeds can bring needless problems. There is another problem related to the capacity, leakage current. This can be generated between two areas, which are unconnected and it can reduce values of useful signals.

7.3 Inductive connection

When current flows through the circuit, constant or alternating electromagnetic field is created around it. When there are conductors in this field, noise voltage U_n is generated. Its value increases when frequency of current's time differences in primary circuit grows. With time difference of magnetic flow Φ, noise voltage according to Faraday's law of induction is

$$U_n = -\frac{d\Phi}{dt} \approx -\frac{\Delta\phi}{\Delta t} = -\frac{\Delta(B \cdot S)}{\Delta t} = -\mu_0 \cdot S \cdot \frac{\Delta H}{\Delta t} \tag{7.1}$$

where U_N is noise voltage, Φ is electron flux, t time derivation, B magnetic induction, μ_0 permeability of vacuum, S cross-section of the conductor and H intensity of magnetic field. When inductive connection is present, current loops must be reduced, also short parallel wires can help. In my case, there was a problem with signals binding between two channels. I was trying to make an area of ground between them and later, I placed there a piece of material with high permeability (in general metals, copper here).

Of course, none of these types of interferences stands itself, in a device there are all of them in various proportions. In the end of this chapter, you can see the results of EMC measuring I did in specialized shielded chamber. They illustrate the differences I got on several board versions and also with use of mentioned high permeability insertion. Witch all the precautions, levels of noise were reduced to 6.33 keV. For measuring of energies beginning at 10 keV, this value is small enough.

8 Testing of XRB board in laboratory conditions

The board was equipped and tested with the courtesy of Mr. Petřík in his workroom in company Dentec. As the source of radiation for testing a sample of Americium was used. Testing included XRB diodes with classical THT montage, SMD diodes, which were finally used in the final flight piece, with and without using of the guard ring. It is very optimistic to expect that we may receive any spectrum from the probe, because now we do not exactly know, which objects and spectrum is possible to recognise with such device. But we want at least find the edge of XRB diodes, test their durability on orbit and the ability to work in different temperatures. To find out how the diodes behave, different kinds of shielding were tested in the laboratory – with a range of materials including the new carbon-fibre, which are testing several tasks on VZLUSat-1. We also tested how much the energy edge of a diode moves, with the change in temperature. All measurements were performed on Cicero 8k unit with the resolution of 8 000 channels. Each channel represents an energy in keV, according to the formula of conversion, (8.1). This formula uses a reference signal from generator which energy is known, or compares energies of two peaks which are defined as well.

$$E_{ch} = \frac{E_2 - E_1}{N_2 - N_1} \tag{8.1}$$

In the simplest case, this formula uses only a reference signal from generator, which energy is known. Thus, E_{ch} corresponds to the energy of one channel, E_2 is energy from signal of generator, N_2 in number of channel where the peak of generator is found and N_1 and E_1 are zero (there is no other signal to compare with). From this equation, energy for one channel was 59.75 eV·chnl^{-1}.

8.1 Tested material

The new carbon-fibre material, which was mentioned several times, was developed by 5M company. During the tests of its shielding qualities, I was testing three different versions of this material. One of them is the material which HM panel is made of too. It is a carbon composite with epoxy matrix, which has reduced content of volatile chemical components and increased radioactivity immunity. The exact

composition of this material I do not know and can not describe, because it is owned by 5M company as a know-how. Carbon fibres are a reinforcement, in HM panel they make 73% of the weight. Metal coating for further enhancement of properties was also applied. There is 50 μm of nickel and it was applied galvanically. There is an additional golden film on one part of the nickel layer, which is 300 nm thick and it was magnetron sputtered. I was testing also two different types of this material, each of them from different years. CFER 2012 does not have the enhanced epoxy matrix, only a standard one, and carbon fibres make 56% of weight. In the year 2013 the same type of resin was used, content of carbon fibres was similar to the 2012 version. There is a difference in boundary layers, which made of the resin in combination with fibres for space use. Flexular modulus of 2013 version was measured and it is 60 GPa.

8.2 Equipment, conditions and apparature

Measuring of parameters was carried out in a laboratory, except cases, which are explicitly mentioned, in standard room temperature and humidity, 25°C and about 65%. The main measuring device was a Cicero 8k unit, a channel spectrometer from Italy (Silena Milano, the company does not exist anymore). All measurements took the same time, 500 s. Data from Cicero were processed by connected laptop into graphs, numbers of channels were converted according to 8.1. Noise and shape of

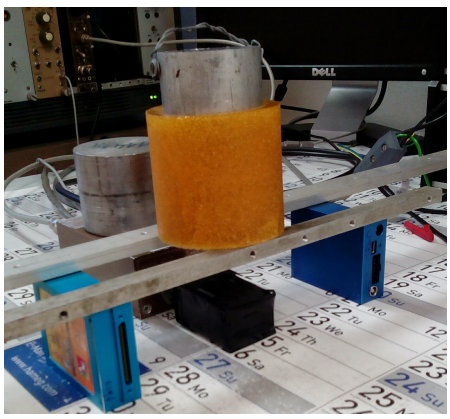

(a) Americium radiator and diode in housing

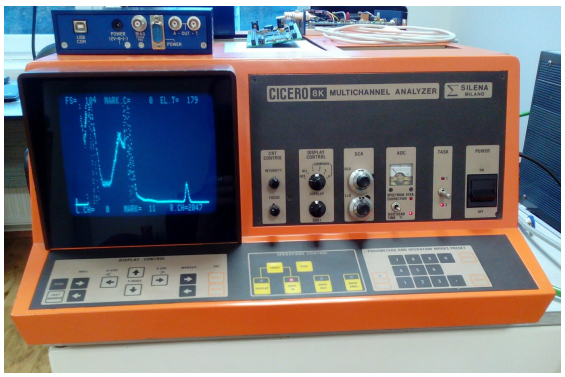

(b) Histogram at Cicero 8k

Fig. 8.1: Measurement station

the signal was observed on oscilloscopes OVON SDS8202 and older analog oscilloscope Tectronix, which helped to determine that one of noise cources was only the

measuring aparature itself. Power source was dual-channel OVON ODP3032., which can provide up to 60 V in serial mode. Distance between the Americium radiator and PIN diode was three centimetres.

8.3 Measuring with weak shielding

The main task of measurement was to compare different kinds of shielding. At first, I wanted to try how sensitive the diodes are to outside effects, like daylight, artificial light. And furthermore, how shall we shield it from these influences to get relevant, undistorted results. So I tried to measure uncovered diode and change the power supply to test where the edge is and what is the effect when the supply rises. As expected, the results were better for higher bias. The diodes can have bias voltage up to 70 V, we measured to 65 V - the value is smaller because we left a reserve for case of lower power losses on amplifier - we did not want to risk damage of the diode. We compared three cases. One is without any shielding, active layer of the diode was exposed to the light of light tubes and daylight in the laboratory.

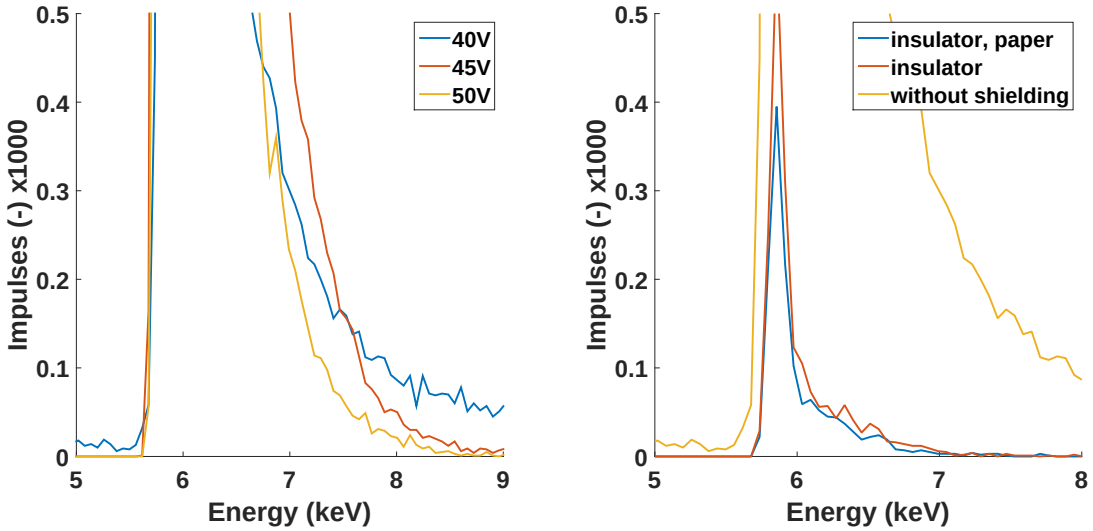

(a) Leakage of the light into sensor's housing (b) Sensor with attenuated influence of room-light

Fig. 8.2: Testing of light influence on XRB diode

This situation caused the error of measurement, there are visible energies too low to be caught by this type of sensor. It was clear that this noise could misrepresent the measurement with radiation shielding, so the whole testing box, including irradiation window, was packed into insulating tape. Then I tried to wrap it into several layers of black paper as well, but as you can see in Fig. 8.2b the difference was minimal, insulating tape itself can eliminate false signals from light.

Then I measured how the edge, noise and false signals will change when I will increase the power supply. In the Fig. 8.3a can be seen that higher biasing voltage in general brings lower noise and better process of the curve. We decided that testing of the materials will be done at biasing voltage 55 V, because this value has low noise, the smoothest shape and it is safe for the device.

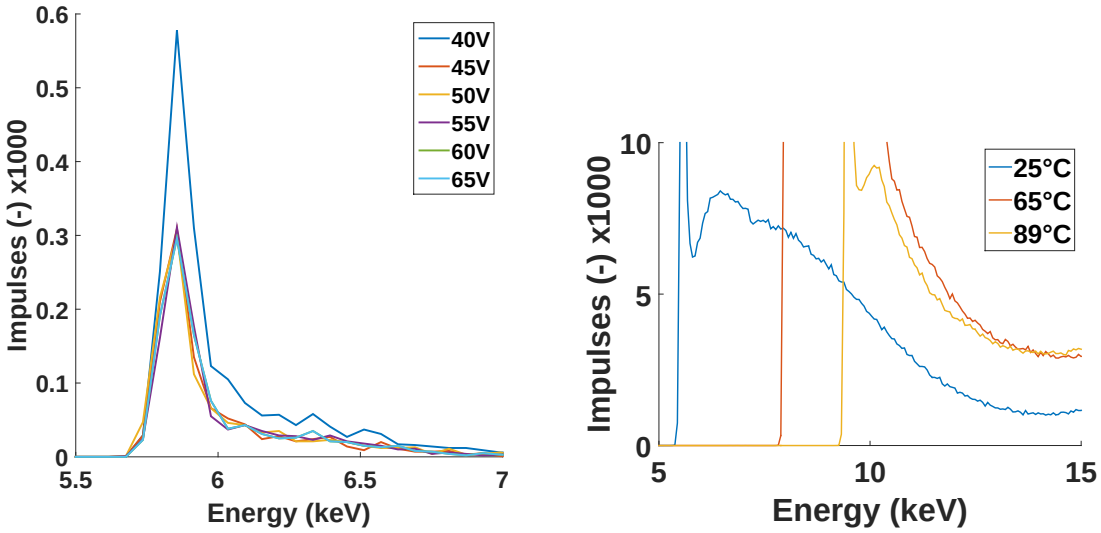

(a) Influence of power supply changes

(b) Influence of rising temperature

Fig. 8.3: Power and temperature influence, insulated housing

Measurement for different temperatures was made as well, and, as illustrated in Fig. 8.3b, the PIN diode will lost its sensitivity of low energies with too high temperature. This problem will be at least partially solved by the Tungsten shield behind the diodes, which will divert a part of the heath away, into the anti-radiation housing and PCB, but its influence will be probably still significant.

8.4 Radiation shields

After the tests of power supply value influence, I proceeded with measurement of shielding by different materials, include the new carbon-fibre by 5M company. In the graph in Fig. 8.4 are compared energies which come through tested materials during 300 s. I was measuring spectrum of Americium radiator, which has to have two main energy peaks, in 26.4 keV and 59.5 keV. The last peak most to the right side of graph is only a reference signal from generator, which is there to help with orientation and ensure that the radiator or measuring system did not move or change its properties accidentally (only in appendices).

I tried to use different materials as a shield, not only carbon-fibre and Tungsten, which will fly. There also is Aluminium, a 1 mm thick layer, as a representative of light metals. It has remarkable lesser atomic number than Tungsten, that means the probability of interaction between radiation and material and from this resulting amount of passing particles is higher. Then there are two types of tested carbon fibre materials, from years 2012 and 2013 with a metal layer of Nickel. CFER from later year has a little better shielding effect.

Most important is, of course, the final tested material by 5M, tagged simply as Carbon. This material, although it is not thicker than the other two CFERs, has significantly better shielding properties. I tried a thin desk of ceramic with $BaTiO_2$ layer as well. This ceramic material was only 0.5 mm thick, this is a reason, why is less shielding effective than lighter, but thicker carbon-fibre material of HM panel.

Just to compare, there are also values got from measuring with Tungsten shield in thickness which will be used as shielding and housing at the probe, and is clear, that in the tested time, Tungsten shielding releases only a minimum of radiation.

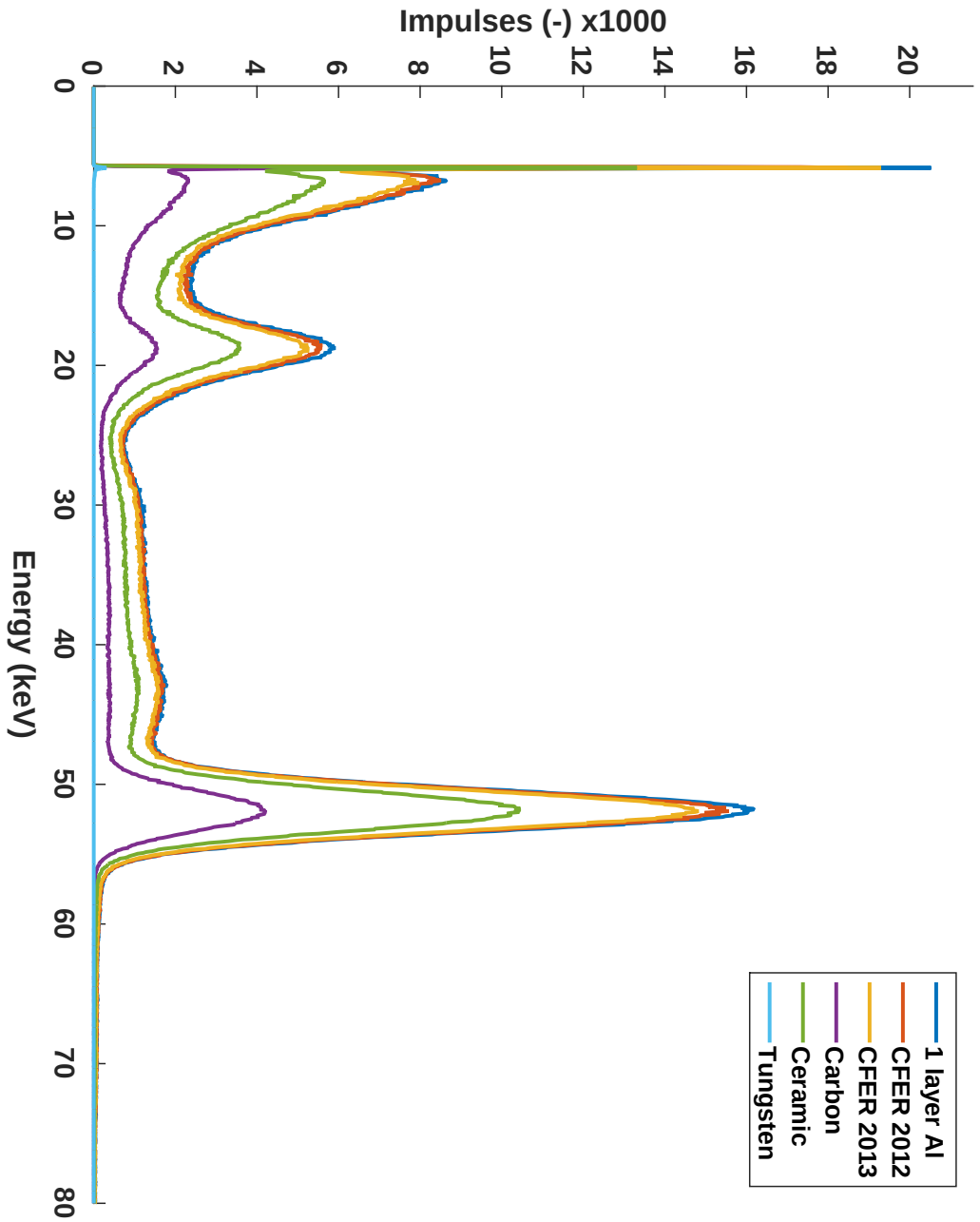

Fig. 8.4: Graph with different shielding materials; 55 V, 25°C

9 Pre-flight tests

Verification of VZLUSat-1 consisted of a row of different tests and simulations. There were applied different scenarios, any payloads were complete, proto-flight models, other were qualification engineering models, devices like batteries were were substituted by dummy, only as a weight. The satellite was completed, inspected and tested, then the tests began.

9.1 Vibrations and shock

The satellite was exposed to random vibrations, sinusoidal vibration and shock waves in mounted axis. After each block of these tests, a resonance search in all axis was done as well. During these tests was found out that some bondings must be made more durable, like wires leading to the Medipix. Also a part of sputtered golden layers was torn.

9.2 Vacuum chamber test

Because the satellite will operate on orbit, it was necessary to test its behaviour in vacuum and also in an appropriate temperature range. The device was placed into a vacuum chamber as can be seen in Fig. 9.1, the chamber was evacuated and functional tests after this process executed. Then were made baking out and temperature cycles for low and high temperature. Followed functional tests again, for minimal and maximal operation temperature as well.

The probe was removed from the vacuum chamber, re-equilibrated in laboratory conditions and final functional tests were done again. In laboratory was normal room temperature, pressure and humidity and the cleanliness was 100 000 particles per m^3.

9.3 EMC testing

After the stress tests followed inspection of probe's state. Then was tested electromagnetic compatibility for radiated emissions in both H and E planes.

During the trials, after each of steps, visual inspection and functional test were performed. In the end, full functional tests were carried out to verify that all the boards are working and communicate across the satellite. [3]

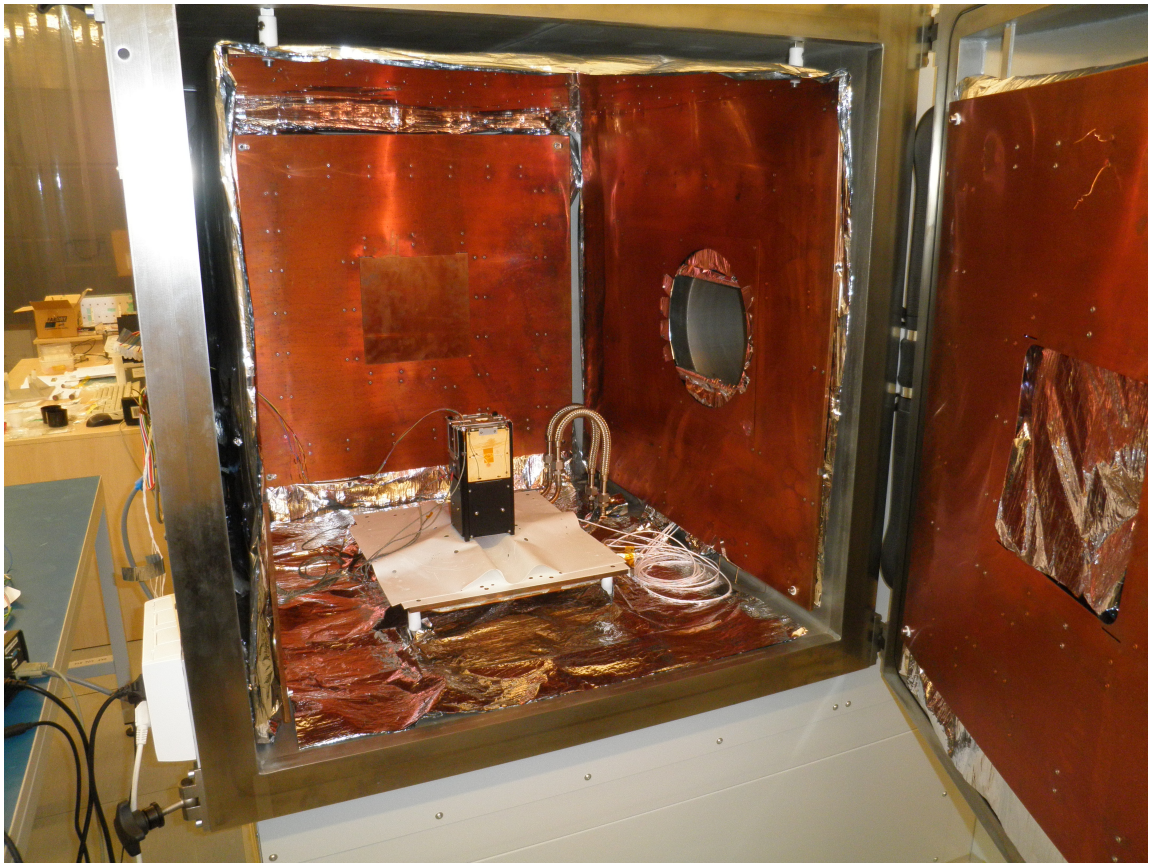

Fig. 9.1: VZLUSat-1 in a vacuum chamber [3]

10 Conclusion

The satellite VZLUSat-1 is a part of QB50 project, dedicated for scientific experiments in the lower thermosphere. This swarm of CubeSats will be launched next year and will examine a series of measurement for improving of atmospheric models of Earth. Besides this task, individual Cubes can carry other scientific units, mainly for testing of new materials and technologies, which are not common in spacecraft nowadays.

VZLUSat-1 will have FIPEX as a part of QB50 requirements on board, then a newly developed carbon-fibre material from company 5M and sensors from TTS and IST will be tested. Experiments will be coordinated by an on-board computed, twice per day the probe will communicate with ground station in Pilsen. In these time windows it is possible to upload new parameters for used commands and new schedule of measurements, and to download obtained results.

One of the experiments on board of VZLUSat-1 is testing of qualities of the new carbon-fibre material when it is applied as a radiation shield. A CdTe detector and three XRB diodes are going to be used for this task. The first diode is equipped with a Tungsten plate, the second one with a carbon-fibre shield and the last one is unshielded. From orbit, we will obtain an individual spectrum for each of these cases. By comparing them, we will be able to assess the damping efficiency of incident radiation.

The main goal of this master's thesis was to design and to test a low-noise analog amplifier for XRB PIN diodes. Expected energies, which the sensors are going to be exposed to on orbit, are beginning at around 10 keV. The value of noise must be low enough for the desired signal from diodes to be still distinguishable. Due to very weak signal from diodes, the risk of cross-talks is high. Also the influence of digital noise from the rest of probe can be malicious. After applying of different methods of noise reduction, the sum of noise of the whole preamplifier was 6.33 keV. This value is sufficient for measurement in expected range of energies and temperatures in the lower thermosphere.

Laboratory tests with wolfram radiator showed that improved formula of epoxy has significantly better properties than formerly used types.

In this thesis, we achieved to design, build and test a radiation measurement board with properties suitable for usage on orbit.

We acknowledge the support provided by TA ČR project TA03011329.

References

[1] BARBOUR, S., ERWIN, D.A. *Comparison of focal properties of square-channel and meridional lobster-eye lenses*. Journal of the Optical Society of America, 2014. ISBN 2584-2592.

[2] Nentvich, Ondřej. *Measurement of changing mechanical properties of carbon composite on nanosatellite miniCube mission QB50*: master's thesis. Prague: Czech Technical University in Prague, Faculty of Electrical Engineering, Department of Micro- electronics, 2015. 73 p. Supervised by Ing. Ladislav Sieger, CSc.

[3] Aerospace Research and Test Establishment, Beranovych 130, Prague

[4] Urban, Martin. *Measurement of evaporation and evaluation of changes of the mechanical properties of carbon composite on nanosatellite miniCube mission QB50*: master's thesis. Prague: Czech Technical University in Prague, Faculty of Electrical Engineering, Department of Micro- electronics, 2015. Supervised by Ing. Ladislav Sieger, CSc.

[5] QB50 - DOCUMENTS [online]. [2015-07-01]. Available from <`https://www.qb50.eu/index.php/tech-docs`>.

[6] Earth's Inconstant Magnetic Field. [online]. 2003-12-29 [2015-06-12]. Available from <`http://www.nasa.gov/vision/earth/lookingatearth/29dec_magneticfield.html`>.

[7] ESA Radiation: Radiation Design Handbook. [online]. Noordwijk: ESA Publications Division, 1993 [2015-04-06]. Available from <`https://escies.org/download/webDocumentFile?id=59313`>

[8] International Space Station: Facts, History & Tracking. [online]. 2015-04-15 [2015-03-19]. Available from <`http://www.aldebaran.cz/tabulky/index.php`>.

[9] ISS tracker - Real-time location tracking of the International Space Station [online]. [2015-03-19]. Available from <`http://www.isstracker.com/`>.

[10] MIR - Wikipedia, the free encyclopedia [online]. [2015-03-19]. Available from <`http://en.wikipedia.org/wiki/Mir`>.

[11] A Weatherman in Space.... [online]. [2015-03-20]. Available from <`http://http://science.nasa.gov/science-news/science-at-nasa/1998/ast29oct98_1/`>.

[12] magnetosphere.jpg. [2015-03-20]. Available from <http://hpde.gsfc.nasa.gov/LWS_Space_Weather/magnetosphere.jpg>.

[13] Colour centre definition - Free Online Encyclopedia. [online]. [2015-05-22]. Available from <http://encyclopedia2.thefreedictionary.com/Colour+centre>.

[14] Aldebaran: Tabulky. [online]. [2015-05-22]. Available from <http://www.space.com/16748-international-space-station.html>.

[15] Bremsstrahlung - European Nuclear Society. [online]. [2015-05-22]. Available from <https://www.euronuclear.org/info/encyclopedia/bremsstrahlung.htm>.

[16] Takahashi, T., Watanabe, S. *Recent Progress in CdTe and CdZnTe Detectors*. Tokio: Institute of Space and Astronautical Science, 2001.

[17] EG&G - Ortec Catalog 1983 - 84, Radiation Detection, Measurement, Analysis. 1983 [2015-07-02]. ORTEC, 100 Midland Road, Oak. Ridge, Tennessee 37830, USA

[18] Milan Petřík, Ing., *Consultations*, Summer 2014-2015, DENTEC, Prague, Czech Republic

[19] ZÁHLAVA, Vít. *Návrh a konstrukce desek plošných spojů: principy a pravidla praktického návrhu*. 1. vyd. Praha: BEN - technická literatura, 2010, 123 s. ISBN 978-80-7300-266-4.

[20] Electromagnetic Spectrum Diagram - MY NASA DATA. [online]. [2015-05-22]. Available from <http://mynasadata.larc.nasa.gov/science-processes/electromagnetic-diagram/>.

[21] HÁNA, P., INNEMAN, A., DÁNIEL, V., et al. Mechanical properties of Carbon Fiber 3 Composites for applications in space. Proc. SPIE 9442, *Optics and Measurement Conference 2014*. 2015, no. 1. DOI: 10.1117/12.2175925.

[22] Kazuo Yana, Ph.D., *Consultations*, Summer 2014, Hosei University, Tokyo, Japan

List of appendices

A Article about VZLUSat-1

Measuring carbon fiber aging on orbit

Bc. Martin Urban[1], Bc. Veronika Stehlikova[1], Bc. Ondrej Nentvich[1], Ing. Ladislav Sieger, CSc.[1] and Kazuo Yana, Ph.D.[2]

[1] Czech Technical University in Prague, Prague, Czech Republic

[2] Hosei University, Koganei City, Tokyo, Japan

- Abstract - **This paper describes the outcome of internship at the faculty of science and engineering, Hosei University in summer 2014. The goal of the project is to design a measuring system of aging properties of a carbon fiber reinforced composite in space. The project is a part of the nano-satellite project at Czech Technical University in Prague, scheduled to be launched in 2016. The measurement environment in space is different from the standard measurements performed on the ground in laboratory. The system design specification has a large constraint in size, weight and power consumption by the limit of space probes. To meet these requirement, the basic measuring system of the mechanical damping characteristics of the carbon fiber composite is designed in this internship project. A damping oscillator to simulate the response of the target material has been assembled and measuring parameters are optimized. The optimized algorithm has been implemented in the chip to be launched on the space orbit.**

I. Project QB50 and probe VZLUSAT1

During our internship at Hosei University we were working on CubeSat project QB50 concretely on the probe VZLUSAT1. This project runs under the auspices of Czech Aerospace Research and Test Establishment (VZLU) and Czech Technical University in Prague (CTU). In this project also cooperates many other companies, for example, Rigaku Innovative Technologies Europe, s.r.o., 5M s.r.o., TTS s.r.o., Innovative Sensor Technology s.r.o., DENTEC and with many other individuals and specialists.

The goal of it is to carry on the orbit a nanosatellite, which will perform diverse experiments. The QB50 project relies on building satellites of defined measures, based on cubes 10x10x10 cm, which can be combined up to three cubes in a row for one probe this time. In the future should be constructed bigger satellites up to 2x2x3 units. Their conformity allows to carry a large number of different probes to the orbit together. The reason of the project's name is, that there will be space for 50 units of two cubes (2U) standardized units aboard. One of each 2U have to had maximum power supply up to 2 Watts and up to 2 kg.

The philosophy of this project is, to make a path for cheaper and easier manufacturing of satellites in the future. To build and carry a satellite to the orbit is not a cheap thing, so it is the reason why even on high-end projects are still used old verified materials and technologies. They simply are proved by time and the project sponsors do not want to risk using any new and untested parts, due to which the whole project could crash.

Compared to these large, separate projects, the SpaceCube program offers an opportunity for lots of scientist, who need to test something new on the orbit without risking lots of funds. These small satellites are carried on next to a main standard satellite, a little bit like a stowaway, which is the carrier primary used for. So these nanosatellites like SpaceCube are depending on projects of standard space research, without the possibility of an independent start. As a small satellite, it does not have own active power also.

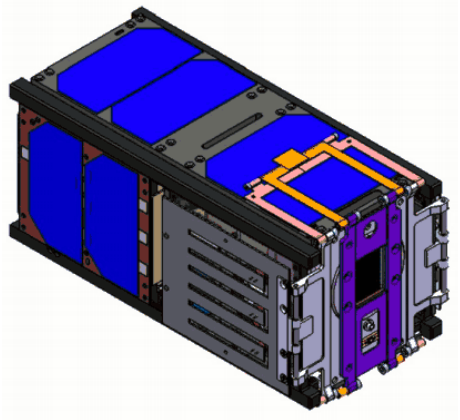

Fig. 1: Appearance of the cube sat VZLUSAT1

In general, the main part of people working on SpaceCubes recruits among the college students and their mentors. It is a chance to work on an interesting project with a possibility of future extension. It is our case too. After the launch, we will cooperate with University of west Bohemia, in Pilsen, where will be the headquarters for communication with orbit. We will get the raw measured data from them that we will process into final results.

II. VZLUSAT1 in general

Project VZLUSAT1 carries ten experiments in total. These experiments have various aims. There are two main tasks on the satellite. One tests a new carbon fiber reinforced composite panel with metallic coating made by 5M and TTS companies for utilization on space probes from the perspective of strength, weight, radiation shielding, durability and evaporation, the second one is Wide-angle X-ray imaging system.

Examining of this composite panel could lead to verification of suitability for this kind of material, which, if it pass, could be used as shielding material for standard satellites e.g. GPS and communication satellites, etc. in the future. Naturally, due to the rising popularity of this cheap nanosatellites like type QB50, this proved material could be used for producing standardized parts of skeleton and shielding for them too. It means an advantage for future experimentators, who will be able to fully concentrate to their research itself, without solving questions of construction and shielding.

Wide-angle X-ray imaging system with Timepix detector is a special type of lens, which works with reflexivity instead of refractivity.

Because the probe doesn't have active engine, there are at least coils for all three dimensions, which will slightly orient the probe in dependence on Earth's magnetic field.

One of next parts of measuring is measuring of humidity. There will be several sensors in the probe, which are connected with the main computer through I^2C. The computer has to be programmed to switch between desired sensors and get measured values.

Last but not least of our tasks is measuring of space radiation and shielding capabilities of composite panel. The probe will have three measuring diodes aboard and they will be shielded by none, one and two layers of composite. This task is complicated due to low sensitivity of diodes in case of high temperatures, and cooling in free space is hard to solve. There also is a problem with additional radiation from inside, from irradiated construction of probe; there will be not only measured signal from space, but this unwanted radiation too. It is necessary to try to separate both environments or subtract it for relevant results.

Space cube carries also many other tasks. For example, there will be sensors for measuring temperature in different parts of probe, or humidity sensors (made by Innovative Sensor Technology s.r.o.), which will measure vaporization rate of tested composite during transition from atmosphere to vacuum. These tasks don't have so high importance and due to the power limitation of whole device they run only when main tasks are switched off, like in case of Timepix doesn't look into the Sun. That means, all tasks are sharing processor time as in time multiplex and have solar and backup battery power together.

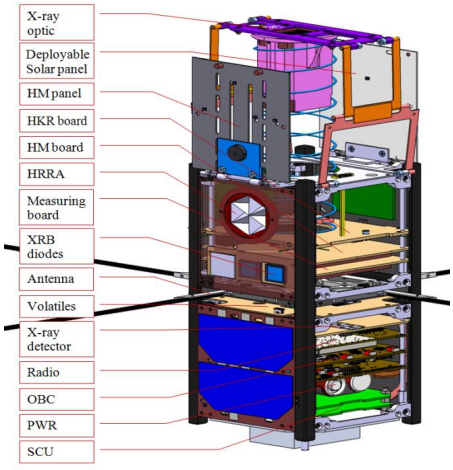

Fig. 2: Measuring boards and inner arrangement

Measured data will be sent to the headquarters in Pilsen when the probe will pass over Czech Republic. It will be approximately twice to day. The speed of data transmission will be changing as well as the time go. Data amount depends on where the probe will be and how long can communicate according to height of orbit where the probe will be. The height of the orbit will reduce over time and data speed will be slower. Due to limited volume of data which is possible to send, is necessary to process raw data on orbit and let to the Earth arrive only results.

Carrier with our VZLUSAT1 will start January 2016 from Brazil, with an Ukraine rocket. It will be brought to low orbit, 350 km high. Then it will collect data at least two month. It depends on how lucky will the probes be during the launch, in case of a great starting angle, it could work half year too. Of course, there are many other possibilities, which can involve lifetime of satellite. It is not sure how well will it deal with temperature changes on orbit, with radiation exposure and other unexpected conditions. Whole time it will send data to the Earth and in the end, space probe will burn in atmosphere.

INTERNSHIP AT HOSEI

I. SUMMARY

Our work comprises technical solution of measuring aging of carbon fiber reinforced composite, and as an usual projects at CTU, it is quite complex. It begins from theory, mathematical and physics modeling and working out the tasks in simulation programs. Then there is a part of trying to apply proposed resolutions on testing facilities, only to check the possibility in real situation. Simulations, include these with high sophisticated software, still cannot cover the entire range of possibilities that may affect the device as a whole. If the device on a breadboard or testing board works, a printed circuit board proposal follows. Last task is to assemble the final version, last testing and then the device can come to mass production or to science use, as in case of our probe.

II. MAIN GOALS OF OUR EXPERIMENT

Whole our work was divided into several parts following one after another. First we had to design printed circuit board for main measuring. This is first step because one testing board must be produced and proved in many tests before the launch. At the moment when design was completed we can start design and write a program for measuring changes in the resonant frequency (due to composite aging).

The main goal is to create and write a program for microcontroller which will measure signal with unknown frequency in range 100-200 Hz (composite material's resonance frequency) by Fast Fourier Transform with the highest possible accuracy in frequency and resolution approximately 0.1 Hz. Another purpose is calculating exponential envelope damping factor. Microcontroller should be able to communicate with on board computer (OBC) via I^2C interface. Next goal is measuring temperature by I^2C thermometer, radiation and evaporation.

Measuring evaporation other gas from the material will ensure by five humidity sensors. These sensors are not only sensitive to humidity but also on some other gases which may be released from the material. To check the will be placed several different types of sensors in the probe. For these sensors was necessary to design the PCB (Printed-Circuit-Board) too.

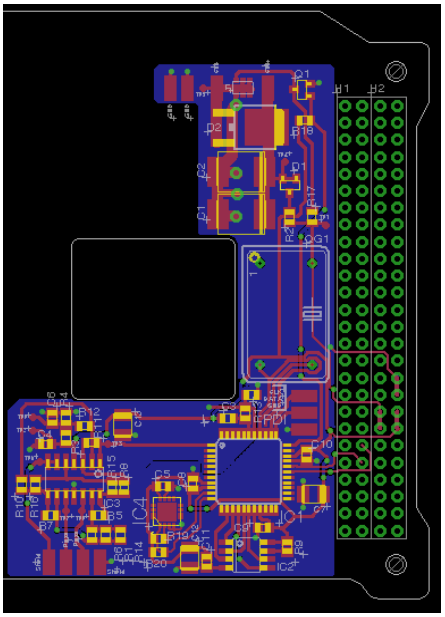

Fig. 3: Printed circuit board for the measurement

III. INPUT SIGNAL

Input signal is measured by piezoelectric element glued on composite plate and has approximately exponential envelope modulated by material resonance frequency. Exponential envelope is caused by attenuation in the material. Useful signal length depends on attenuation, which is caused by physical dimensions and material properties in the material and amount of energy excited by coil. In the picture fig. 4 is shown one example of input signal. Measured real signal has total length 0.9 s.

Input signal is sampled by 8 kHz. In case of computing attenuation (envelope) is used all signal for the better resolution in time. This signal is averaged by moving averages. Smoothed result is logarithmed and attenuation is directive of the course.

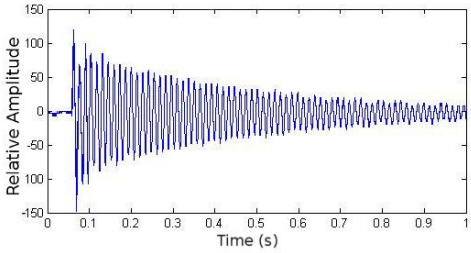

Fig. 4: Measured real damped signal

Resonance frequency is computed from decimated original signal using Fast Fourier Transform. If we use only FFT on the original signal we can calculate only with 1024 points (length of window) because we are limited by memory size installed in the probe. Computing by this process has final resolution more than several Hertz. What is a reason why we used decimation from 8 kHz to 500 Hz? The result of resolution is sufficient for us up to 200 Hz and sample frequency 500 Hz passed Shannon-Nyquist sample theorem with enough reserve.

This theorem says minimal sampling frequency must be two times higher than maximal measured sampled frequency.

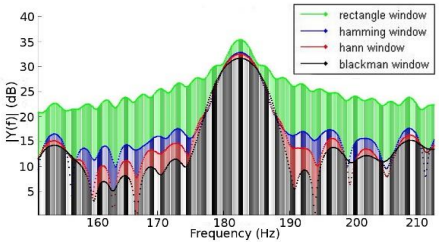

Fig. 5: FFT results with window length 4096 samples and different types of windows

Results for FFT with signal sampling 500 Hz and window length 1024 are better than previous one, resolution is 0.5 Hz, but it is still not enough. (Required is approx. 0.1 Hz.) This limit of calculation allowed us to save memory and to use larger window. We made interpolation with help of adding zeros behind the signal into expanded window with window length 4096 points. Resolution of the decimated signal to 500 Hz with these calculation parameters is approx. 0.12 Hz according to formula (1). Implemented measurement in the program aboard the probe, must sample signal just only once, so it leads to choose higher sampling rate and then apply decimation on signal to requested sampling rate. All these computations were simulated in MATLAB.

$$\Delta f = \frac{f_s}{n} \qquad (1)$$

IV. Calculation process

Main process consists of several functions. Here is a brief list:

Sampling and storing data

The analog to digital converter included in microcontroller could sample signal up to two million samples per second. So it leads to averaging four-points groups to eliminate glitches. All data are stored into SPI SRAM memory from which are further loaded.

Computing damping envelope

First what is needed to do is to perform mathematically absolute value to get one sided envelope. Next step is logarithming signal because it is needed to get attenuation, which represents *b* in exponential expression as shown in formula (2). Then is applied moving averages to smooth signal and computing directive using least squares method.

$$f = A \cdot e^{-\mathrm{bt}} \qquad (2)$$

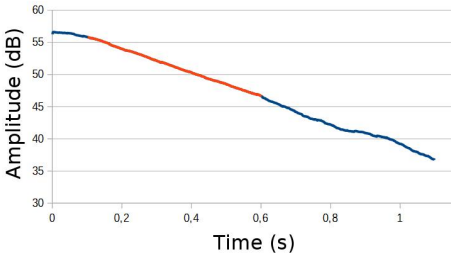

Fig. 6: Attenuation computed by least squares

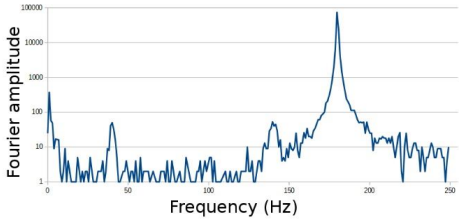

Fig. 7: FFT result by development kit

Computing Fast Fourier Transform

It is known, that resonance frequency of new material is in range 100-200 Hz so the signal sampled by 8 kHz must be decimated to 500 Hz to observe condition of the highest accuracy in frequency. FFT algorithm decimation in time is calculated in two steps. First step is to swap sampled points according to address which is bit reversed and next step is calculating Fast Fourier Transform. Program performs decimation and bit-reversing simultaneously. Program chooses one point and stores it to the bit-reversed address into SPI memory. Right address positions are stored in the table. Computation process picks up two points from memory, performs FFT algorithm and stores new points on the original positions. After that program finds the highest peak which corresponds with resonant frequency.

Store results into memory for further dispatch to the Earth

Results of attenuation and resonance frequency are stored into internal EEPROM memory of microcontroller for further dispatch to the Earth. Memory can include data amount which corresponds 40 hours of recording and hold data also after power loss.

V. Functionality Verification

During writing a program for development kit was necessary to check all functions. It leads to create device which one generates approximately the same signal as it gets from oscillations on the probe. With this idea came professor Yana who provided us draft of schematic, which is redrawn by Eagle software illustrated in the picture fig. 8.

The circuit produces oscillations with exponential envelope. To the circuit must be connected external oscillator as input of the board.

The board consists of some parts as monostable gate, output is connected to analog multiplier through capacitor which produces exponential envelope. To the multiplier is also brought external oscillator. Both inputs are multiplied in integrated circuit AD633. Output is connected to adder with another input from potentiometer which provide DC offset. Output of the board should be DC shifted in range +/- 15V. The board has power supply +5V and converted to +/-15V through DC/DC converter. Output voltage damped oscillations depends on voltage of oscillator and envelope.

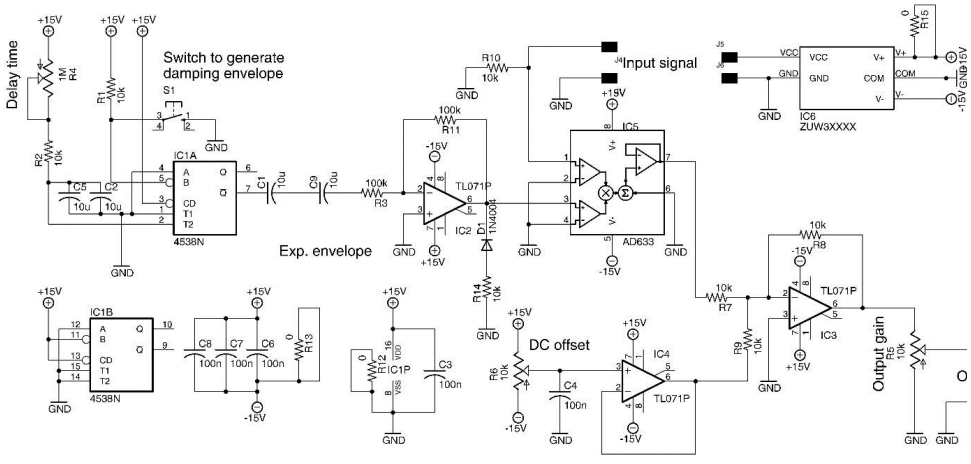

Fig. 8: Damping exponential envelope generator - schematic

Final board is in the picture fig. 9. Professor Yana was benevolent and arranged produce at manufacturer who create some pieces of boards which we assembled from parts who gave us. We are very pleased to create and then testing on it damping oscillations measured by development kit.

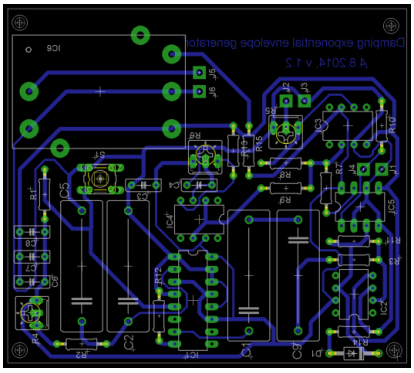

Fig. 9: Damping exponential envelope generator – Printed circuit board

The whole board was assembled and tested under supervision and technical assistance of Mr. Saitoh and Mr. Iki. They kindly provided us their laboratory with all necessary equipment like oscilloscope, signal generator or soldering station. Final assembled board is in the picture fig. 10.

Fig. 10: Assembled damping oscillator

VI. Conclusion

During our internship we collaborated mainly with professors Kazuo Yana, Gaku Minorikawa and Akira Yasuda. These professors helped us to realize internship and during the whole summer helped us not only with the project but with staying in Japan too. Thanks to them we have progressed with our project and got great experience of Japan too.

Project VZLUSAT1 with cooperation VZLU consists of many measurements. One is measuring of material aging in the space. Measurement consists of exciting carbon fiber reinforced composite material by coil and measuring vibration by piezoelectric element. Damped signal with exponential envelope is sampled by microcontroller and then are calculated resonance frequency and damping factor. Using mentioned process is possibly to get final frequency resolution approx. 0.12 Hz. Every results as resonance frequency and damping factor as humidity and radiation are stored into memory and then are dispatch to the Earth during contact twice per a day.

Space probe CubeSat with name VZLUSAT1 will by launched in January 2016 and is funded by grants Technology Agency of the Czech Republic TA04011295 and TA03011329.

Acknowledgement

Authors wish to thank Professors Minorikawa, Ohsawa with the department of Mechanical Engineering and Professor Yasuda with the department of Electrical and Electronic Engineering, Hosei University for their encouragement. Authors also wish to thank Mr. Saitoh and Iki with the department of applied informatics, Hosei University for their technical support.

References

[1] Wide-angle X-ray imaging system with Timepix detector, RIGAKU, project number TACR TA04011295, 7/2014-12/2017
[2] Experimental verification for space products and technologies on nanosatellite VZLUSAT1, project number TACR TA03011329
[3] Cooperation and consultation with Czech Aerospace Research and Test Establishment
[4] Ing. L. Sieger, CSc., consultations, Czech Technical University in Prague, Prague, Czech Republic
[5] K. Yana, Ph.D., consultations, Hosei University, Tokyo, Japan
[6] RNDr. P. Hána, CSc., consultations, Technical University of Liberec, Liberec, Czech Republic
[7] Prof. Ing. P. Sovka, CSc., Studying material for subject "Digital Signal Processing", Czech Technical University in Prague, Prague, Czech Republic 2013/2014
[8] "Decimation-in-time (DIT) Radix-2 FFT", summer 2014, [on-line] <http://cnx.org/contents/ce67266a-1851-47e4-8bfc-82eb447212b4@7>
[9] Datasheets for used parts

Contacts

M. Urban, urbanm24@fel.cvut.cz
V. Stehlikova, stehlver@fel.cvut.cz
O. Nentvich, nentvond@fel.cvut.cz

B Additional graphs

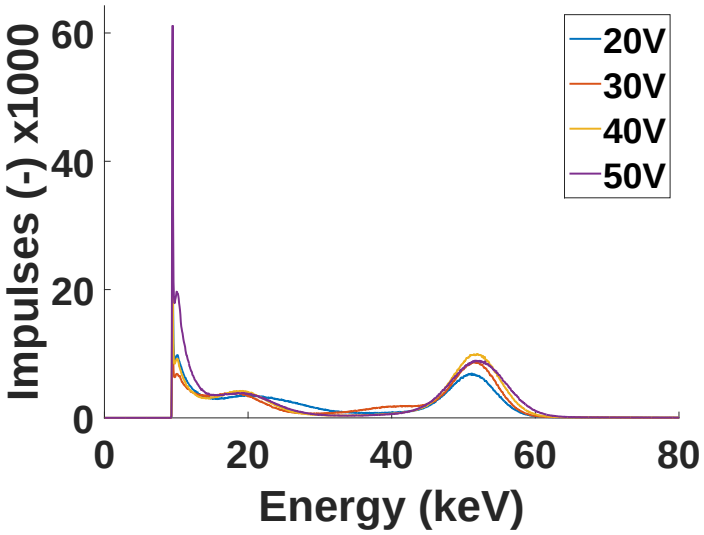

Fig. B.1: Different voltages, 89°C

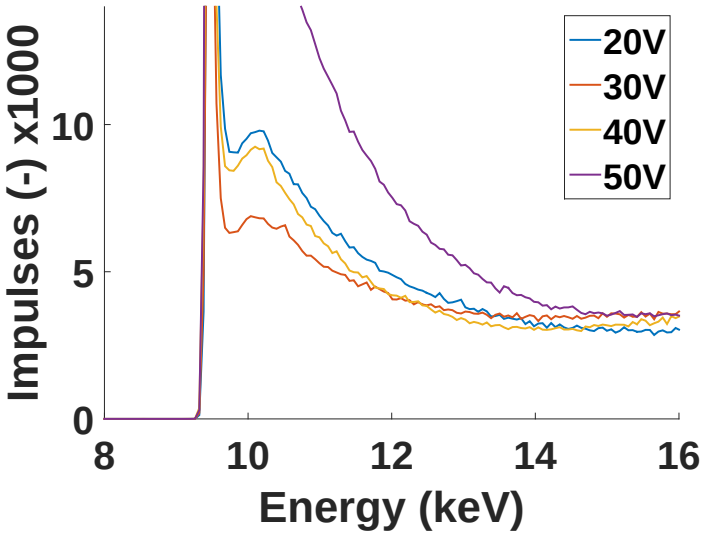

Fig. B.2: Different voltages, 89°C, detail

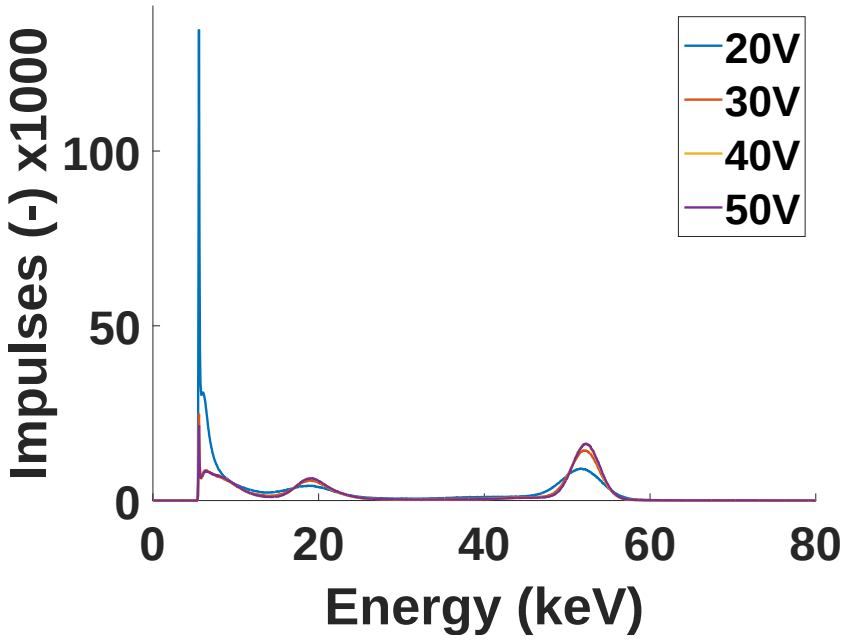

Fig. B.3: Different voltages, 25°C

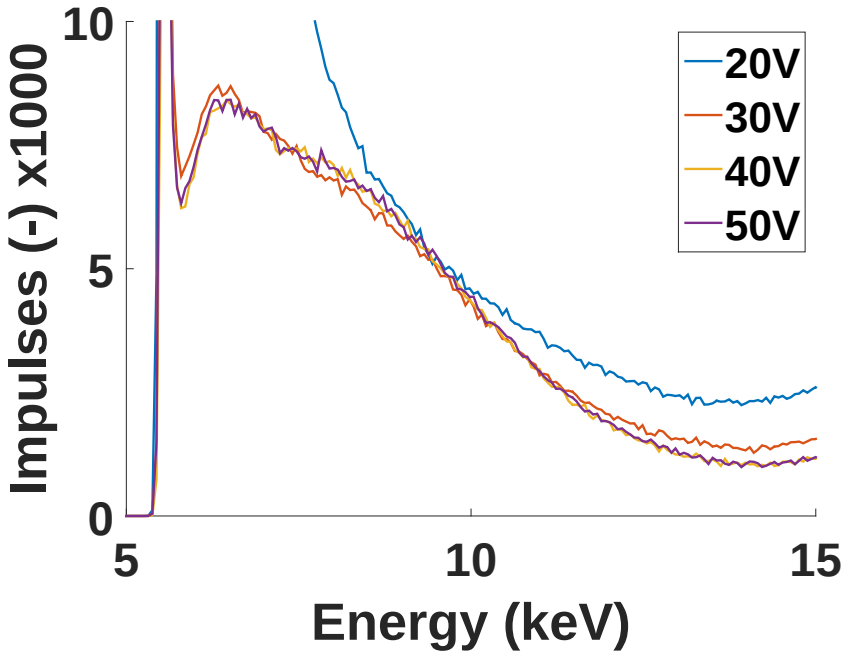

Fig. B.4: Different voltages, 25°C, detail

C DVD content

Measured data, datasheets of used particles, any articles and pictures, layouts, master's thesis